

Fast Byte Latent Transformer

Julie Kallini^{1,2}, Artidoro Pagnoni¹, Tomasz Limisiewicz^{1,3}, Gargi Ghosh¹, Luke Zettlemoyer^{1,3}, Christopher Potts², Xiaochuang Han¹, Srinivasan Iyer¹

¹FAIR at Meta, ²Stanford University, ³University of Washington

Recent byte-level language models (LMs) match the performance of token-level models without relying on subword vocabularies, yet their utility is limited by slow, byte-by-byte autoregressive generation. We address this bottleneck in the Byte Latent Transformer (BLT) through new training and generation techniques. First, we introduce **BLT Diffusion (BLT-D)**, a new model and our fastest BLT variant, trained with an auxiliary block-wise diffusion objective alongside the standard next-byte prediction loss. This enables an inference procedure that generates multiple bytes in parallel per decoding step, substantially reducing the number of forward passes required to generate a sequence. Second, we propose two extensions inspired by speculative decoding that trade some of this speed for higher generation quality: **BLT Self-speculation (BLT-S)**, in which BLT’s local decoder continues generating past its normal patch boundaries to draft bytes, which are then verified with a single full-model forward pass; and **BLT Diffusion+Verification (BLT-DV)**, which augments BLT-D with an autoregressive verification step after diffusion-based generation. All methods may achieve an estimated memory-bandwidth cost over 50% lower than BLT on generation tasks. Each approach offers its own unique advantages, together removing key barriers to the practical use of byte-level LMs.

Date: May 11, 2026

Correspondence: Julie Kallini at kallini@stanford.edu, Srinivasan Iyer at sviyer@meta.com



1 Introduction

Byte-level (also known as *tokenizer-free*) language models operate directly on raw bytes rather than a predefined vocabulary of tokens. By avoiding subword tokenization, they address several well-known shortcomings of token-level models, including sensitivity to input noise (Pruthi et al., 2019; Sun et al., 2020), handling structured or out-of-domain inputs (Dagan et al., 2024; Singh and Strouse, 2024; Zhou et al., 2024), limited character-level understanding (Kaushal and Mahowald, 2022; Huang et al., 2023; Edman et al., 2024), and multilingual disparities (Ahia et al., 2023; Petrov et al., 2023; Liang et al., 2023). Despite their many advantages, byte-level models have seen limited adoption relative to subword models. The core issue is efficiency: since a typical subword token spans several bytes, a naively autoregressive byte-level model must operate over sequences that are many times longer than their token-level counterparts, dramatically increasing both training and inference cost (Xue et al., 2022).

Recent architectural innovations have substantially narrowed this efficiency gap. Rather than running a full Transformer over every byte, modern byte-level models often group bytes into larger units, use hierarchical computation, or replace full attention with more efficient sequence modeling mechanisms (El Boukkouri et al., 2020; Clark et al., 2022; Tay et al., 2022; Nawrot et al., 2022, 2023; Yu et al., 2023; Slagle, 2024; Wang et al., 2024; Kallini et al., 2025; Zheng et al., 2025; Pagnoni et al., 2025; Hwang et al., 2025). For example, the **Byte Latent Transformer** (BLT; Pagnoni et al. 2025) dynamically groups bytes into variable-length *patches* based on input complexity. Its hierarchical design concentrates computation on *latent token* representations, allocating more compute to complex patches of text and yielding better scaling behavior than token-level models.

These advances reduce the *compute* cost of byte-level models, but inference still faces a *memory bandwidth* bottleneck. In modern LLM inference, generation cost is often dominated by repeatedly loading model weights and accessing key-value caches (Pope et al., 2023; Kwon et al., 2023; Yuan et al., 2024). Even when most computation is performed over latent token representations, standard byte-level decoding still generates one byte at a time. Since a typical subword token corresponds to several bytes, an autoregressive byte-level

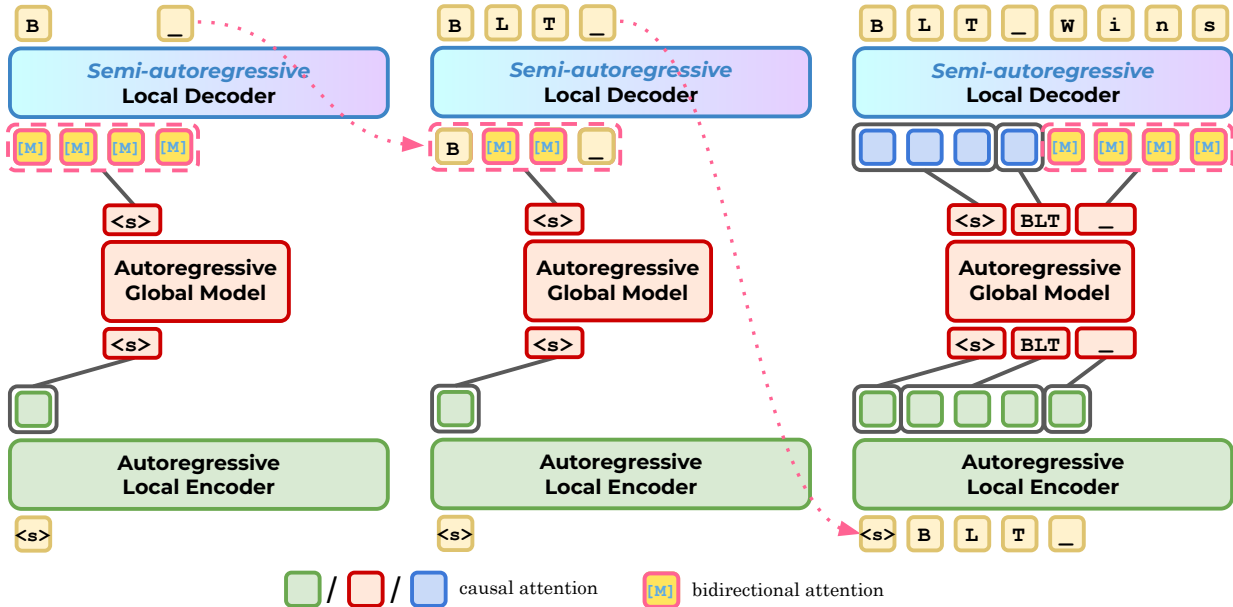


Figure 1 BLT-D inference. The encoder creates latent token representations from variable-length patches of bytes. The large global model predicts the next latent token. The decoder initializes a fixed-length block of [MASK] tokens and generates bytes in parallel via semi-autoregressive text diffusion, conditioning on the last latent token. **Compared to BLT, this inference approach decreases the forward passes/network function evaluations (NFEs) of all model components (encoder, global model, and decoder).**

model such as BLT requires multiple decoder forward passes to generate the same amount of text represented by a single subword token. This paper targets that bottleneck. Our goal is to enable byte-level parallel generation while preserving the main benefits of BLT: operating directly on bytes, using dynamic patching, and concentrating computation in latent token representations.

We first draw inspiration from diffusion language models (dLMs), which improve decoding efficiency by generating multiple tokens in parallel within a single forward pass (Sahoo et al., 2024; Lou et al., 2024; Wu et al., 2025; Nie et al., 2025; Arriola et al., 2025), reducing memory bandwidth per generated byte. However, existing text diffusion methods are not directly designed for byte-level architectures whose latent tokens are constructed dynamically from variable-length patches. This creates a key challenge: the model must generate future bytes in parallel while remaining compatible with BLT’s dynamic, hierarchical architecture.

We introduce **BLT Diffusion (BLT-D)** (Figure 1), a new byte-level model that combines BLT’s hierarchical latent tokenization with block-wise discrete diffusion. BLT-D retains BLT’s local encoder and global model structure, but modifies training and decoding so that the local decoder can generate a fixed-size block of future bytes in parallel. During training, BLT-D’s decoder receives both a clean byte sequence and a corrupted sequence of fixed-length byte blocks. These blocks are constructed from dynamically segmented patches but can extend beyond individual patch boundaries, allowing the decoder to learn to predict future bytes beyond the average BLT patch size. The decoder is trained with a combined objective: the standard autoregressive next-byte prediction loss on clean bytes, and a masked-byte prediction loss on corrupted byte blocks. At inference time, BLT-D initializes a block of masked byte positions and iteratively unmask multiple positions per decoder step, conditioning on the most recent latent representation. This reduces the number of required decoder, encoder, and global model evaluations per generated sequence.

BLT-D offers the largest speedups, but diffusion-based generation introduces a quality–efficiency trade-off. Larger diffusion blocks can reduce inference cost dramatically, because more bytes are generated per decoder call, but they also require the model to predict farther into the future without fully autoregressive conditioning, which can degrade generation quality. To address this, we introduce two additional inference extensions inspired by speculative decoding (Leviathan et al., 2023; Zhang et al., 2024; Cai et al., 2024). Unlike prior speculative decoding methods that typically use a separate draft model or additional speculative layers, our

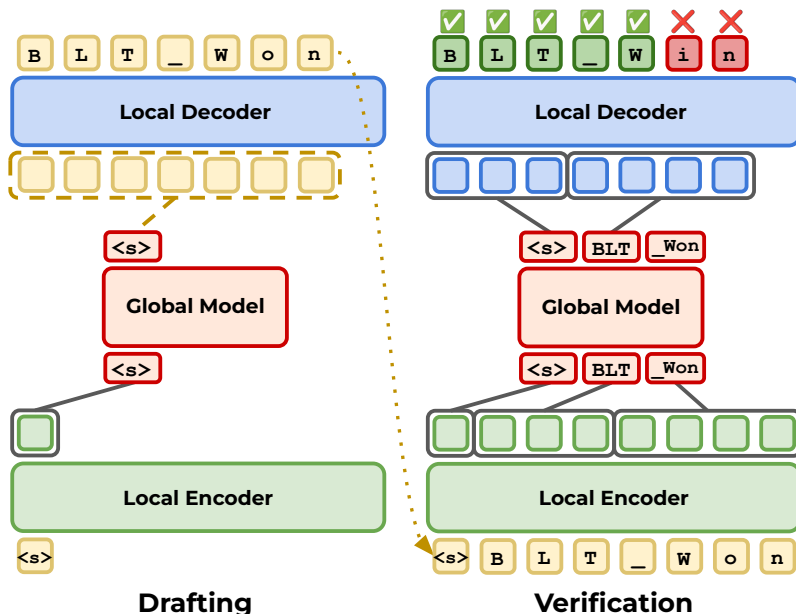


Figure 2 Verification procedure shared by BLT-S and BLT-DV. After a block of bytes is drafted (via self-speculation in BLT-S or diffusion in BLT-DV), the full model re-encodes the candidate sequence and produces next-byte predictions using causal attention. Drafted bytes are accepted up to the first mismatch, which is replaced with the model’s prediction. Under greedy decoding, this guarantees that verified outputs are identical to standard autoregressive decoding.

methods exploit the existing hierarchical structure of BLT and BLT-D (Figure 2).

The first extension is **BLT Self-speculation (BLT-S)**. In standard BLT generation, the local decoder stops generating whenever the entropy-based patcher determines that a new patch should begin. BLT-S instead allows the lightweight decoder to autoregressively draft several bytes beyond the usual patch boundary. The full BLT model then verifies this draft using a normal forward pass. If the drafted bytes match the model’s verified predictions, they are accepted; otherwise, generation rolls back to the first mismatch and continues from the verified byte. BLT-S therefore reduces the number of expensive encoder/global calls while preserving the output of standard autoregressive BLT decoding. Unlike conventional speculative decoding, BLT-S does not require a separate draft model: the existing local decoder acts as the drafting mechanism.

The second extension is **BLT Diffusion+Verification (BLT-DV)**. BLT-D is trained not only with a diffusion objective but also with a standard next-byte prediction objective, so the same model can be run autoregressively with causal decoder masks. BLT-DV uses this fact to combine fast diffusion drafting with autoregressive verification. The diffusion decoder first proposes a block of bytes, and the model then verifies the proposed block using next-byte predictions. This improves generation quality relative to diffusion-only BLT-D while retaining much of the speedup from block-level drafting. BLT-DV therefore occupies a middle point in the trade-off: it is slower than pure BLT-D but typically stronger in task performance.

Contributions This paper makes three main contributions:

1. We introduce **BLT-D**, a byte-level language model that makes block-wise discrete diffusion compatible with BLT’s dynamic patching and hierarchical latent representations, enabling parallel byte generation without fixed subword tokenization.
2. We propose two verification-based inference extensions: **BLT-S**, which accelerates standard BLT using its own decoder as a draft mechanism, and **BLT-DV**, which improves BLT-D generation quality by verifying diffusion drafts with autoregressive next-byte predictions.
3. We empirically characterize the speed–quality trade-offs of these methods at 1B and 3B parameter scales across translation and code generation tasks. We provide additional likelihood-based evaluations and generation-diversity analyses.

Across our experiments, BLT-D is our fastest model and inference method, achieving over 50% lower estimated memory-bandwidth cost compared to BLT on translation and code generation tasks. With larger diffusion block sizes, BLT-D may achieve up to 92% reduction, with some degradation in task performance. BLT-DV recovers some of this performance while still achieving up to 81% reduction compared to BLT, and BLT-S achieves up to 77% reduction with no loss in task performance. Overall, each of these methods has its own unique advantages and helps to further close the inference efficiency gap between byte-level and subword-level models.

2 Background and Related Work

In this section, we provide background on BLT and diffusion language models. We further discuss speculative decoding in [Section 5](#), where we introduce our extensions.

2.1 Byte Latent Transformer

BLT is a byte-level architecture that operates directly on raw byte sequences while matching the performance of subword tokenization-based language models at scale. BLT dynamically groups bytes into variable-length *patches*, which serve as the primary units of computation. Patches are constructed using an entropy-based segmentation strategy driven by next-byte uncertainty estimated by a small auxiliary byte-level language model. Given a byte input sequence $x = [x_1; x_2; \dots; x_N] \in \mathcal{V}^N$ of length N , where \mathcal{V} is a small byte vocabulary, the sequence is split into $M \approx \frac{N}{4}$ variable-length patches $[p_1; p_2; \dots; p_M]$. High-entropy regions are segmented into shorter patches, while more predictable spans are grouped into longer patches, thus controlling how frequently the resource-heavy global model is invoked.

2.1.1 Architecture overview

BLT’s architecture creates latent token representations that mix byte- and patch-level information. It consists of three components: a local encoder \mathcal{E} , a global transformer \mathcal{G} , and a local decoder \mathcal{D} . The local encoder embeds the length- N byte input x to create initial byte representations $\mathbf{X} = [\mathbf{x}_1; \mathbf{x}_2; \dots; \mathbf{x}_N] \in \mathbb{R}^{N \times d_{\text{local}}}$, where d_{local} is the hidden dimensionality of the local encoder and decoder modules and where \mathbf{x}_i is the embedding of byte x_i . The encoder then processes \mathbf{X} into M latent token representations $\mathbf{T} = [\mathbf{t}_1; \mathbf{t}_2; \dots; \mathbf{t}_M] \in \mathbb{R}^{M \times d_{\text{global}}}$, where d_{global} is the hidden dimensionality of the global model. The global Transformer then maps \mathbf{T} to output latent token representations $\mathbf{O} = [\mathbf{o}_1; \mathbf{o}_2; \dots; \mathbf{o}_M] \in \mathbb{R}^{M \times d_{\text{global}}}$. Since our method modifies the decoder, we omit further details of \mathcal{E} and \mathcal{G} and refer the reader to [Pagnoni et al. 2025](#).

2.1.2 Local decoder

The local decoder \mathcal{D} autoregressively decodes the final latent token representations \mathbf{o} into a sequence of output bytes $y = [y_1; y_2; \dots; y_N] \in \mathcal{V}^N$ using $L_{\mathcal{D}}$ lightweight Transformer layers. At each layer, byte-level hidden states are updated via cross-attention to latent token representations before applying a standard Transformer layer. Let $\mathbf{D}_l = [\mathbf{d}_{l,1}; \mathbf{d}_{l,2}; \dots; \mathbf{d}_{l,N}] \in \mathbb{R}^{N \times d_{\text{local}}}$ denote the byte hidden states of a length- N byte sequence output by layer l of the decoder, with $\mathbf{D}_0 \in \mathbb{R}^{N \times d_{\text{local}}}$ being the initial representations from an embedding lookup for y . For each decoder layer $l \in \{1, \dots, L_{\mathcal{D}}\}$, the cross-attention from byte hidden states to latent token representations is computed as

$$\mathbf{B}_l = \mathbf{D}_{l-1} + \mathbf{W}_o \left(\text{softmax} \left(\frac{\mathbf{Q}\mathbf{K}^\top}{\sqrt{d_k}} \right) \mathbf{V} \right), \quad (1)$$

where $\mathbf{Q}_i = \mathbf{W}_q(\mathbf{d}_{l-1,i})$, $\mathbf{K}_j = \mathbf{W}_k(D_C(\mathbf{o}_j))$, and $\mathbf{V}_j = \mathbf{W}_v(D_C(\mathbf{o}_j))$. Here, d_k is the dimensionality of the key vectors for a single attention head. \mathbf{W}_q , \mathbf{W}_k , and \mathbf{W}_v are the query, key, and value projection matrices, $D_C(\cdot)$ denotes a linear transformation and splitting function applied to latent token representations, and \mathbf{W}_o is the output projection. The cross-attention does not use positional encodings. The updated byte representations are then produced by

$$\mathbf{D}_l = \text{DecoderTransformerLayer}(\mathbf{B}_l). \quad (2)$$

The decoder Transformer layer employs multi-head attention, pre-LayerNorm, and RoPE positional encodings.

2.2 Diffusion Language Models

Diffusion models define generative distributions by progressively corrupting data through a forward noising process and learning a reverse process that iteratively removes noise. Recent work extends this framework to discrete domains such as text by defining stochastic corruption processes over token sequences, enabling training of diffusion language models (dLMs) with diffusion-style objectives and generation over discrete tokens (Austin et al., 2021a; Campbell et al., 2022; Li et al., 2022; Gulrajani and Hashimoto, 2023; Lou et al., 2024). These models are typically non-autoregressive, employing bidirectional attention over all tokens, or semi-autoregressive, using bidirectional attention within fixed-length blocks while maintaining causal dependencies across blocks (Arriola et al., 2025; Gat et al., 2025). Here, we focus on absorbing discrete diffusion with conventions similar to those presented by Ye et al. (2025) and Nie et al. (2025), which is conceptually very similar to masked language models (Devlin et al., 2019).

2.2.1 Absorbing Discrete Diffusion

We draw a clean text sequence $x^0 = [x_1^0; x_2^0 \dots; x_N^0] \in \mathcal{V}^N$ from the data distribution, where \mathcal{V} is the vocabulary and N is the sequence length. We define a discrete diffusion process based on random input masking: given x^0 , we sample a continuous diffusion timestep (noise level) $t \sim \mathcal{U}(0, 1)$ and independently replace each position with a special [MASK] token with probability t , producing a corrupted sequence x^t . The forward corruption distribution q is

$$q(x_i^t = [\text{MASK}] \mid x_i^0) = t, \quad q(x_i^t = x_i^0 \mid x_i^0) = 1 - t, \quad (3)$$

with independence across positions. Prior work has shown that this masking process can be interpreted as the marginal of a discrete diffusion model with an absorbing state, where [MASK] is absorbing and t controls the diffusion time.

We parameterize a denoising model $p_\theta(x_i^0 \mid x^t, t)$ that predicts the original token values at masked positions, conditioned on the partially observed sequence and the noise level. Training minimizes the weighted denoising objective

$$\mathcal{L}(\theta) = -\mathbb{E}_{x^0, t, x^t} \left[\frac{1}{t} \sum_{i=1}^N \mathbb{1}_{[x_i^t = [\text{MASK}]]} \log p_\theta(x_i^0 \mid x^t, t) \right], \quad (4)$$

which has been shown to correspond to a simplified evidence lower bound (ELBO) on the data log-likelihood, or equivalently, an upper bound on the negative log-likelihood (Shi et al., 2024; Gong et al., 2025). Following Ye et al. (2025) and Nie et al. (2025), we do not embed the timestep t into the architecture directly and instead assume that it is implicitly encoded through the input data corruption.

3 BLT Diffusion

BLT achieves scalable and efficient byte-level modeling by dynamically allocating compute resources through hierarchical latent tokenization. However, inference speed remains a significant bottleneck, as traditional autoregressive generation proceeds one byte at a time. BLT-D directly addresses this challenge by introducing block diffusion decoding in a way that is fully compatible with BLT’s hierarchical architecture, reducing model calls and therefore memory bandwidth at inference. We adapt the absorbing diffusion framework from Section 2.2 to operate over fixed-size blocks within BLT’s decoder.

3.1 BLT-D Inference

BLT-D inference decodes a fully masked block in parallel in much fewer iterations than autoregressively generating a byte at a time (Figure 1). BLT-D’s encoder \mathcal{E} and global model \mathcal{G} operate exactly like BLT, as described in Section 2.1. Given a length- N prefix $x = [x_1; \dots; x_N] \in \mathcal{V}^N$, the patcher segments x into M variable-length patches. The encoder \mathcal{E} produces byte embeddings $\mathbf{X} \in \mathbb{R}^{N \times d_{\text{local}}}$ and encodes them into latent token representations $\mathbf{T} = [\mathbf{t}_1; \dots; \mathbf{t}_M] \in \mathbb{R}^{M \times d_{\text{global}}}$. The global model \mathcal{G} outputs contextual latent tokens $\mathbf{O} = [\mathbf{o}_1; \dots; \mathbf{o}_M] \in \mathbb{R}^{M \times d_{\text{global}}}$.

Algorithm 1 BLTDGeneration($x, L, B, \text{do_verify}$)

Input: Initial byte sequence $x = [x_1; \dots; x_N]$; generation length L ; block size B ; boolean do_verify
 $l \leftarrow |x|$
while $l < N + L$ **do**
 Patch Encoding:
 Segment x into M patches via entropy-based patcher
 $\mathbf{T} \leftarrow \mathcal{E}(x)$; $\mathbf{O} \leftarrow \mathcal{G}(\mathbf{T})$
 Block Diffusion Decoding:
 $x_{\text{block}} \leftarrow \{\text{[MASK]}\}^B$
 $x' \leftarrow [x_1; \dots; x_l; x_{\text{block}}]$
 while x' contains [MASK] **do**
 $y \leftarrow \mathcal{D}(x'; \mathbf{O})$ ▷ Bidirectional self-attention for block positions
 Select $1 \leq k \leq B$ block positions to unmask ▷ EB sampling or confidence-based
 Replace selected [MASK] positions in x' with predictions from y
 end while
 if do_verify **then**
 $x \leftarrow \text{Verify}(x, x', l, B)$
 else
 $x \leftarrow x'$
 end if
 $l \leftarrow |x|$
end while
Output: Generated sequence x of length $\geq N + L$

For block diffusion inference, the decoder \mathcal{D} receives as input both the latent token representations \mathbf{O} and a byte sequence $x' = [x_1; \dots; x_N; x_{N+1}; \dots; x_{N+B}] \in \mathcal{V}^{N+B}$, where $[x_{N+1}; \dots; x_{N+B}] = \{\text{[MASK]}\}^B$ form a block of B masked positions. \mathcal{D} iteratively computes forward passes over x' until the entire block of B bytes is unmasked. See [Algorithm 1](#) for a more detailed description of the generation procedure.¹ The subsequent sections detail the inference attention patterns and block unmasking strategies used during generation.

3.1.1 Attention Patterns

Let $i \in \{1, \dots, N + B\}$ index positions in x' . Let $p(i)$ denote the patch index for position i in x' . For the decoder’s cross-attention module, for clean positions in the sequence ($i \leq N$), each position attends to the latent token $\mathbf{o}_{p(i)-1}$ corresponding to the previous patch, except for the final byte of each patch, which attends to its own latent token $\mathbf{o}_{p(i)}$ (consistent with BLT). For positions in the masked block ($i > N$), all positions attend to the last latent token \mathbf{o}_M . For \mathcal{D} ’s self-attention, the attention mask $A \in \{0, 1\}^{(N+B) \times (N+B)}$ is defined as follows. For prefix positions ($i \leq N$), \mathcal{D} ’s self-attention is causal: $A_{ij} = 1$ if $j \leq i$. For block positions ($i > N$), self-attention is fully bidirectional: $A_{ij} = 1$ for all $j \leq N + B$. We provide a visualization of these inference attention masks in [Figure 3](#).

3.1.2 Block Unmasking Strategy

The choice of which bytes to unmask at each decoder forward pass affects both the generation quality and the degree of parallelism. We consider two unmasking strategies that differ in how they select masked positions for decoding.

Confidence-based Unmasking The first strategy is confidence-based unmasking ([Ghazvininejad et al., 2019](#)). At each decoder step, the model predicts a distribution over the byte vocabulary for each masked position, and we measure confidence using the maximum predicted probability. All masked positions whose confidence exceeds a threshold α are decoded in parallel, while lower-confidence positions remain masked for subsequent

¹The do_verify branch is used for BLT-DV, introduced in [Section 5](#); for BLT-D, $\text{do_verify} = \text{False}$.

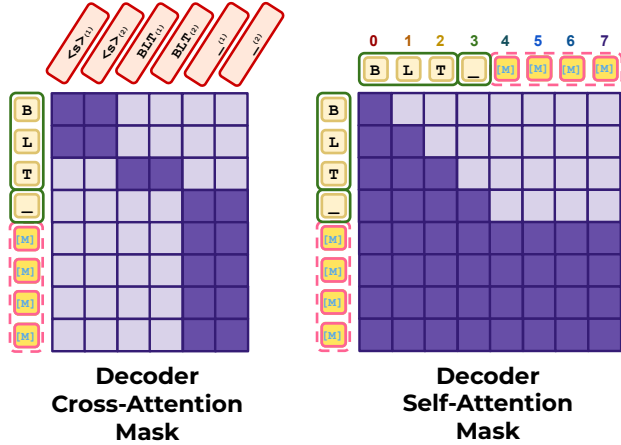


Figure 3 BLT-D attention masks during generation with block diffusion. Before cross-attention, latent tokens are first split into multiple representations via a linear transformation and splitting function (described in detail in Pagnoni et al. 2025). Within the cross-attention, each byte attends to the representations of the previous latent token, except for the last byte of a patch, which may attend to its own latent token. In the self-attention, the clean prefix uses causal attention, and the corrupted/masked portion of the sequence uses bidirectional attention.

steps. This approach prioritizes high-certainty predictions. If no position satisfies the threshold, the highest-confidence position is unmasked to ensure progress.

Entropy-bounded Sampling The second strategy is entropy-bounded (EB) sampling (Ben-Hamu et al., 2025; Gat et al., 2025). At each decoder step, we compute the entropy of the predicted distribution for each masked token and sort masked positions in ascending order of entropy. Since mutual information among masked tokens is intractable to compute directly, we use an upper bound based on marginal entropies and select the largest subset of positions whose cumulative entropy does not exceed a threshold γ . The selected tokens are decoded in parallel, while the remaining tokens remain masked. This unmasking strategy may be combined with top- p sampling to obtain diverse generations from the model. Like confidence-based unmasking, if no position satisfies the threshold, the lowest-entropy position is unmasked to ensure progress.

3.1.3 Speedup

Compared to standard autoregressive decoding, this approach reduces the number of decoder forward passes: generating a block of size B requires s unmasking steps rather than B sequential steps. Usually, $s < B$, which results in a speedup. Additionally, the encoder and global model are invoked less frequently, as these components are called once per block—typically larger than the average patch—rather than at every new patch. Furthermore, the clean prefix and the first $M - 1$ latent tokens from \mathcal{E} , \mathcal{G} , and \mathcal{D} can be cached, with only the final latent token and drafted block requiring recomputation.

3.2 BLT-D Training

BLT-D uses a new training method that enables byte diffusion decoding over latent tokens using specific training data preprocessing, special attention masking in its decoder, and a new loss function. These additions enable BLT-D to predict diffusion blocks that span future bytes far beyond BLT’s typical patch size.

3.2.1 Training Data Preprocessing

To enable block-wise masked prediction, we preprocess each training example as follows. We are given an input byte sequence $x = [x_1; x_2; \dots; x_N] \in \mathcal{V}^N$ (where \mathcal{V} is a small byte vocabulary), segmented into M variable-length patches with patch p_i starting at index s_i .² We construct blocks of bytes and noise these blocks

²Patch p_1 is one byte, and is excluded from block construction.

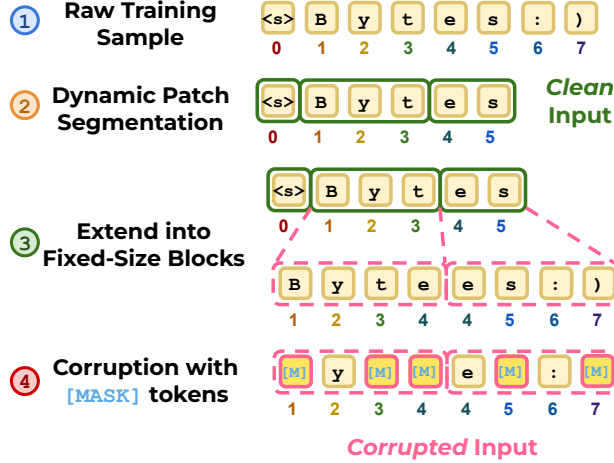


Figure 4 BLT-D training data preprocessing. (1) A raw training sample is loaded. (2) The entropy patcher segments the input dynamically; for illustration, only the first three patches are shown. This is referred to as the *clean* input. (3) All patches except the first are expanded into fixed-size blocks, containing bytes from future patches, with the original positional indices preserved. Allowing predictions beyond the patch enables BLT-D to draft beyond its average patch size during inference. (4) The blocks are corrupted with [MASK]s, resulting in the *corrupted* input.

with diffusion, as described in the next paragraphs. For reference, Figure 4 visualizes this data preprocessing for a short example with block size $B = 4$.

Block Construction From x , we construct a corresponding sequence x_{block} consisting of $M - 1$ fixed-length blocks of size B . For each patch p_i (excluding the first), we define block b_{i-1} as the B consecutive bytes starting at index s_i ; that is, for $i \in \{2, \dots, M\}$, $b_{i-1} = [x_{s_i}; x_{s_i+1}; \dots; x_{s_i+B-1}] \in \mathcal{V}^B$. Since we typically configure B to be greater than the average patch size, these blocks often extend into positions beyond their corresponding patch. This enables BLT-D to predict bytes beyond its average patch size during inference. If a block extends beyond the end of the sequence ($s_i + B - 1 > N$), we pad it to length B with a special token (e.g. [PAD]). All blocks are concatenated to form the sequence $x_{\text{block}} = [b_1; b_2; \dots; b_{M-1}] \in \mathcal{V}^{B \cdot (M-1)}$. For each block b_{i-1} , we record the original byte positional indices $[s_i; s_i + 1; \dots; s_i + B - 1]$. These are concatenated for RoPE positional encodings in the decoder during training, ensuring each byte retains representations based on its original position.

Diffusion Process and Masking To simulate the diffusion process, we sample a continuous timestep $t \sim \mathcal{U}(0, 1)$ and independently replace each byte of x_{block} with a [MASK] token with probability t , to produce $x_{\text{block}}^t \in \{\mathcal{V} \cup [\text{MASK}]\}^{B \cdot (M-1)}$. This produces a partially masked input for the model to reconstruct. We refer to the original sequence x as the *clean* sequence, and x_{block}^t as the *corrupted* sequence.

3.2.2 Decoder Architecture and Attention Patterns

The primary architectural innovation in BLT-D lies in the local decoder \mathcal{D} , which enables block diffusion decoding. A detailed visualization of the architecture during a training forward pass is shown in Figure 5. BLT-D initializes the decoder input \mathbf{D}_0 from embeddings of the concatenated clean and corrupted sequences: $\mathbf{D}_0 = \text{Embed}([x; x_{\text{block}}^t])$.

For each byte in \mathbf{D}_0 , cross-attention is applied to the corresponding output latent token in \mathbf{O} . Clean sequence positions associated with patch p_i cross-attend to the previous latent token \mathbf{o}_{i-1} , except final bytes, which attend to their own latent token \mathbf{o}_i , consistent with BLT. Corrupted sequence positions associated with patch p_i cross-attend to the previous latent token \mathbf{o}_{i-1} . This pattern maintains the alignment between patches and blocks throughout the sequence. Self-attention in \mathcal{D} uses a causal mask for the clean sequence and bidirectional attention within each block of the corrupted sequence. Each byte within a given block in the corrupted sequence also attends causally to all previous clean bytes. RoPE positional encoding uses the

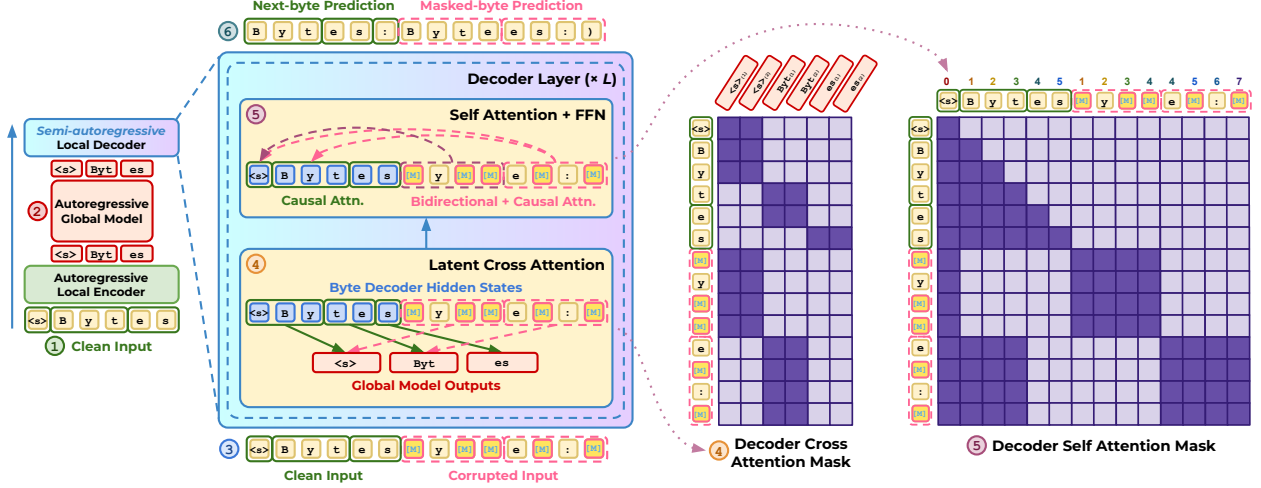


Figure 5 BLT-D training forward pass. (1-2) The encoder and global model process the clean input. (3) Clean and corrupted inputs are concatenated and passed to the decoder. (4) Byte hidden states cross-attend to their corresponding latent representations from the global model. (5) For the clean portion, self-attention is causal; for the corrupted portion, self-attention is bidirectional within each block, and causal towards previous clean patches. (6) Next-byte prediction loss is computed for the clean sequence, and masked byte prediction/diffusion loss is computed for corrupted sequence.

original positional indices as we defined previously.

3.2.3 Loss Function

We use a loss function that combines next-byte prediction on the clean sequence with masked reconstruction on the corrupted sequence. First, recall the clean sequence $x = [x_1; \dots; x_N] \in \mathcal{V}^N$, segmented into M patches with starting indices s_i . We compute an autoregressive next-byte prediction loss:

$$\mathcal{L}_{\text{clean}}(\theta) = - \sum_{i=1}^N \log p_{\theta}(x_i | x_{<i}) \quad (5)$$

Here, $p_{\theta}(x_i | x_{<i})$ denotes the model’s predicted probability of byte x_i given the prefix $x_{<i}$. Next, recall the corrupted sequence $x_{\text{block}}^t = [b_1^t; \dots; b_{M-1}^t]$. Each corrupted block $b_{i-1}^t = [x_{s_i}^t; x_{s_i+1}^t; \dots; x_{s_i+B-1}^t] \in \{\mathcal{V} \cup [\text{MASK}]\}^B$ for $i \in \{2, \dots, M\}$, with each byte masked with probability t . For each corrupted block b_{i-1}^t , let $b_{i-1,k}^t$ denote the k -th byte of the block. The masked diffusion loss is:

$$\mathcal{L}_{\text{mask}}(\theta) = - \frac{1}{t} \sum_{i=2}^M \sum_{k=0}^{B-1} \mathbb{1}_{[b_{i-1,k}^t = \text{MASK}]} \log p_{\theta}(x_{s_i+k} | b_{i-1}^t, x_{<s_i}) \quad (6)$$

where $\mathbb{1}_{[b_{i-1,k}^t = \text{MASK}]}$ is an indicator function that is 1 if the k -th byte of block b_{i-1}^t is masked, and 0 otherwise. The model reconstructs the clean byte x_{s_i+k} , conditioned on the partially masked block and the clean prefix preceding the block, consistent with the self-attention masking pattern described above. The scaling by $1/t$ follows the absorbing discrete diffusion loss discussed previously in [Section 2.2](#).

The total training loss is the sum of the clean sequence loss and the masked diffusion loss:

$$\mathcal{L}_{\text{total}}(\theta) = \mathcal{L}_{\text{clean}}(\theta) + \mathcal{L}_{\text{mask}}(\theta) \quad (7)$$

This combined objective encourages the model to learn both autoregressive next-byte prediction and robust reconstruction of masked bytes in block-wise corrupted sequences.

4 Pre-training and Generation Experiments

In this section, we detail the architectures and hyperparameters of each BLT and BLT-D model we train, as well as the pre-training dataset and optimization settings. We evaluate our models on four generation tasks and discuss the efficiency metrics and results.

4.1 Models, Pre-training Data, and Optimization

We pre-train four model types: one BLT and three BLT-D variants with block sizes of 4, 8, and 16, referred to as BLT-D-4, BLT-D-8, and BLT-D-16, respectively. For each model type, we train both 1B- and 3B-parameter versions. Our 1B BLT and BLT-D models consist of a global model with 1.28 billion parameters, a local encoder with 19 million parameters, and a local decoder with 160 million parameters. Our 3B BLT and BLT-D models include a global model with 2.82 billion parameters, a local encoder with 26 million parameters, and a local decoder with 160 million parameters. All models employ entropy patching, using an average patch size of 4 bytes and a maximum patch size of 8 bytes. To ensure comparability, all models are trained on the BLT-1T dataset from [Pagnoni et al. 2025](#), which consists of 1 trillion tokens collected from various public sources and includes a subset of the pre-training data released by Datacomp-LM ([Li et al., 2024](#)). For additional details on model implementation, hyperparameters, and pre-training optimization settings, see [Section A](#).

4.2 Generation Tasks, Settings, and Metrics

We evaluate our BLT and BLT-D models on four generation tasks: two translation tasks and two coding tasks. For translation, we evaluate French-to-English and German-to-English (4-shot) using the FLORES-101 benchmark ([Goyal et al., 2022](#)), with performance measured by SentencePiece BLEU. For coding, we assess models on HumanEval (0-shot) ([Chen et al., 2021](#)) and MBPP (3-shot) ([Austin et al., 2021b](#)), reporting `pass@1` scores. All task-evaluation inference uses greedy decoding. For BLT-D models, we experiment with both confidence-based unmasking and entropy-bounded sampling as diffusion unmasking strategies, conducting hyperparameter sweeps for each.

Efficiency is evaluated using three metrics: (1) the average number of decoder network function evaluations (NFEs, or forward passes) per output sequence; (2) the average number of encoder/global model NFEs per output sequence; and (3) an estimate of the memory bandwidth required for parameter memory loads during evaluation. The total memory bandwidth, measured in gigabytes, is calculated as follows:

$$\frac{b [N_{\text{dec}} \cdot P_{\text{dec}} + N_{\text{enc}} \cdot (P_{\text{enc}} + P_{\text{glob}})]}{10^9} \quad (8)$$

Here, N_{dec} and N_{enc} represent the average number of function evaluations for the decoder and encoder/global model, respectively. P_{dec} , P_{enc} , and P_{glob} denote the number of parameters in the decoder, encoder, and global model. The variable b specifies the number of bytes required to represent each parameter; in our calculations, we set $b = 2$ to reflect 16-bit precision. This formulation assumes that evaluations are performed with a small KV cache and batch size, so the memory bandwidth is dominated by loading model weights. Small batch sizes are common in local serving and latency-oriented applications, where execution speed is prioritized over batching efficiency. BLT-D supports KV caching, and therefore benefits from any techniques that reduce KV-cache memory footprint. Alternatively, memory bandwidth may be interpreted as a weighted function of NFEs for each model component.

4.3 Generation Task Results

We present the performance of our 3B models across a range of generation tasks, as illustrated in [Figure 6](#). For clarity and brevity, this section focuses on representative BLT-D models utilizing confidence-based unmasking as the diffusion generation strategy, with a confidence threshold of $\alpha = 0.7$. For comprehensive results for both 1B and 3B model variants, including full inference hyperparameter sweeps using both confidence-based unmasking and EB sampling strategies, please refer to [Section B](#) and [Section C](#).

Across all evaluated tasks, BLT-D models consistently outperform BLT in terms of efficiency. Specifically, BLT-D variants achieve substantial reductions in both decoder NFEs and encoder/global NFEs, resulting in

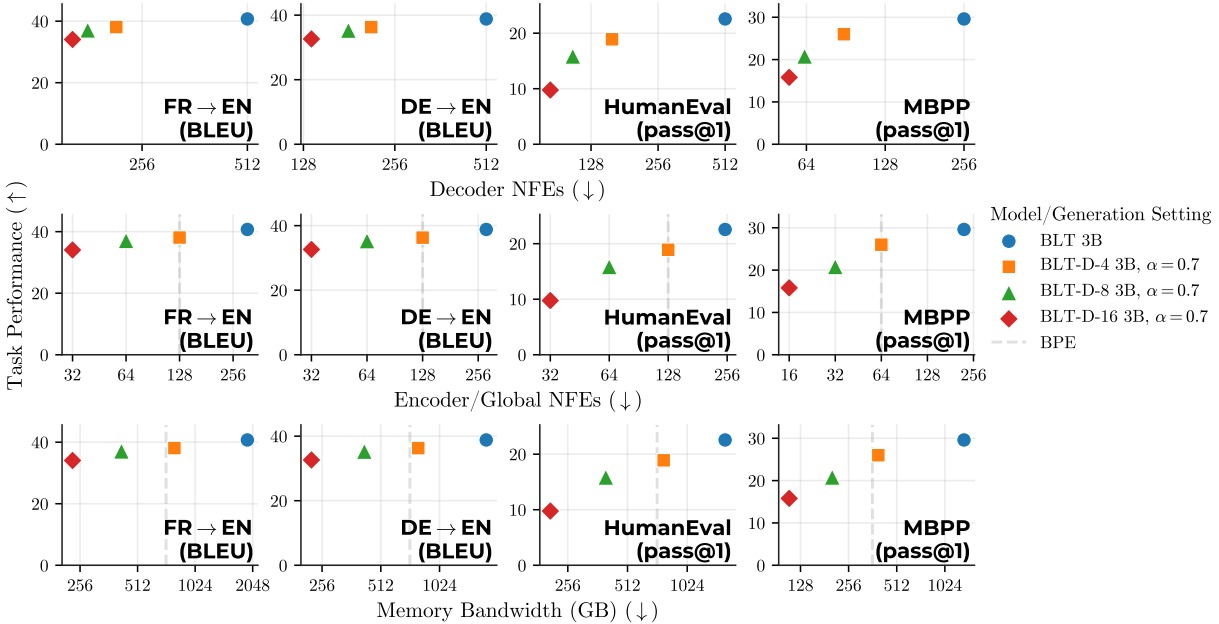


Figure 6 Generation task results of 3B-parameter variants of BLT, BLT-D-4, BLT-D-8, and BLT-D-16. Higher is better for task performance; lower is better for NFEs and memory bandwidth. The NFEs and memory bandwidth for a byte-pair encoding (BPE) model matching BLT’s global model size are shown as a dashed line. BLT-D models are substantially faster than BLT while maintaining strong task performance, especially for translation. BLT-D-16 offers the most efficiency, with reduced performance on the coding-related tasks.

large memory bandwidth decreases. For example, BLT-D-4 nearly matches BLT’s task scores while requiring less than half the NFEs and memory bandwidth. Both BLT-D-4 and BLT-D-8 demonstrate strong task performance with great gains in efficiency, especially on the translation tasks.

Increasing the block size in BLT-D models (e.g., BLT-D-16) leads to even greater reductions in NFEs, highlighting the scalability of this approach. BLT-D-16 achieves an 87–92% reduction in memory bandwidth compared to BLT, making it the fastest model in our evaluations. However, while BLT-D-16 remains competitive on translation tasks, its enhanced efficiency comes at the expense of lower performance on coding-related tasks. This suggests a trade-off between speed and generation quality as block size increases. These results highlight the versatility of BLT-D models, enabling fast generation while allowing flexibility to adjust the block size to suit specific application needs.

5 Extensions: BLT-S and BLT-DV

Based on our observations from the previous section, BLT achieves strong task performance but suffers from slow generation, while BLT-D greatly improves efficiency but can lose quality at larger block sizes. To improve both models, we draw inspiration from speculative decoding, which accelerates autoregressive generation by separating decoding into a fast *drafting* stage and a slower *verification* stage (Leviathan et al., 2023). In standard speculative decoding, a lightweight *draft model* proposes multiple future tokens, and the large *target model* verifies those proposals in parallel, accepting a prefix of the draft while preserving the target model’s output distribution. Subsequent work has reduced the need for a separate draft model by using self-speculation or additional speculative heads (Zhang et al., 2024; Cai et al., 2024).

Our setting is different: BLT and BLT-D already decompose generation into lightweight byte-level decoding and more expensive encoder/global-model computation. We therefore use the existing model components themselves as drafters: BLT-S drafts with BLT’s local decoder beyond normal patch boundaries, while BLT-DV drafts with BLT-D’s diffusion decoder and verifies with autoregressive next-byte prediction. These

Algorithm 2 $\text{Verify}(x, x', l, r)$

Input: current sequence x ; candidate sequence x' ; start index l ; draft length r
Segment x' into M' patches via entropy-based patcher
 $\mathbf{T}' \leftarrow \mathcal{E}(x')$; $\mathbf{O}' \leftarrow \mathcal{G}(\mathbf{T}')$; $y \leftarrow \mathcal{D}(x'; \mathbf{O}')$ $\triangleright y_j$ denotes the greedy next-byte prediction after position j
 $i \leftarrow l + 1$
while $i \leq l + r$ **do**
 if $x'_i \neq y_{i-1}$ **then**
 $x_i \leftarrow y_{i-1}$ \triangleright Reject drafted byte; replace first mismatch
 break
 else
 $x_i \leftarrow x'_i$ \triangleright Accept drafted byte
 end if
 $i \leftarrow i + 1$
end while
if $i = l + r + 1$ **then**
 $x_i \leftarrow y_{i-1}$ \triangleright No mismatches; use free byte from next-byte prediction
end if
Output: updated sequence x

inference extensions require no architectural changes or additional training.

5.1 BLT Self-speculation

We introduce a new approach to enhance BLT’s inference efficiency by enabling its decoder to speculate beyond where it would normally segment patches. In standard BLT inference, the entropy-based patcher halts generation whenever a high-entropy byte is produced, prompting a new invocation of the encoder and compute-intensive global model. This patching typically occurs every four bytes. Instead of immediately patching at each high-entropy byte, we propose a self-speculative decoding strategy, which we call **BLT-S (BLT Self-speculation)**. Here, the decoder always autoregressively generates up to a fixed window size k regardless of entropy spikes, conditioning on the last available latent token. After producing a draft of k bytes, the patcher segments the sequence and computes a full forward pass through \mathcal{E} , \mathcal{G} , and \mathcal{D} to obtain new predictions. The model compares the drafted text to these predictions: if all bytes match, the draft is committed; if not, only the bytes up to the first mismatch are accepted. This iterative process advances by at least one verified byte per step and continues until the target sequence length is reached.

In our setup, verification requires an exact byte-wise match between drafted bytes and the model-verified bytes, and we only evaluate with greedy decoding. This procedure is inspired by speculative decoding but differs in that we validate the bytes themselves rather than their probability distributions; this makes our acceptance criteria stricter than standard speculative decoding. However, our setup is fully compatible with rejection sampling with different temperatures, but we leave explorations of these settings to future work. See [Algorithm 2](#) for a detailed verification procedure.

Our method fundamentally differs from previous speculative decoding techniques, which typically employ a separate small model or additional layers for self-verification ([Leviathan et al., 2023](#); [Zhang et al., 2024](#); [Cai et al., 2024](#)). In contrast, BLT-S leverages BLT’s existing lightweight decoder (\mathcal{D}) for drafting, without introducing auxiliary models or new architectural overhead. By allowing the decoder to generate longer speculative windows, BLT-S increases the number of decoder NFEs, but reduces encoder and global model NFEs, leading to improved inference efficiency overall.

5.2 BLT Diffusion+Verification

Recall that the total training loss in [Equation \(7\)](#) includes $\mathcal{L}_{\text{clean}}$, the standard autoregressive loss. Since BLT-D is trained with a next-byte prediction objective, it can be run autoregressively using the same causal decoder masks as BLT. At inference time, the only adjustment needed is to apply the same decoder self-attention and cross-attention masks used in BLT. This design enables a new generation paradigm for

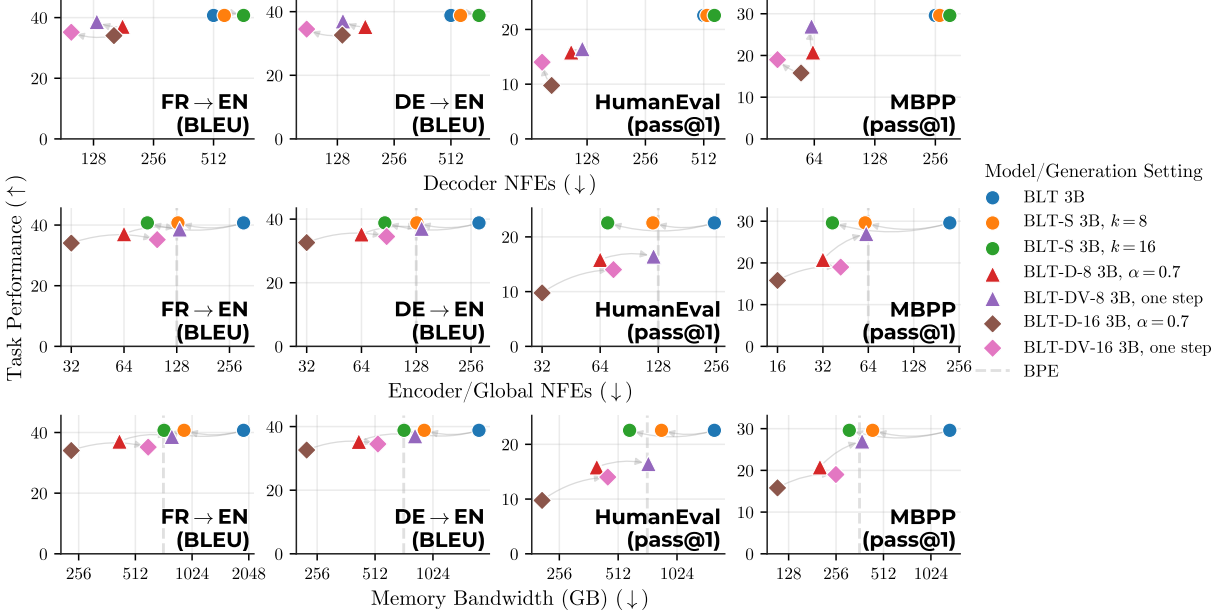


Figure 7 Generation task results for 3B-parameter variants of BLT, BLT-S, BLT-D, and BLT-DV. For space, we report results only for $k \in \{8, 16\}$ and $B \in \{8, 16\}$. Arrows indicate the same model evaluated with different inference methods. Verification (BLT-DV) enhances the task performance of BLT-D models, but increases global NFEs and memory bandwidth. Self-speculation (BLT-S) greatly improves BLT’s speed, with no loss in task performance. BLT-D remains the fastest model/inference method overall.

BLT-D, where diffusion acts as the drafting mechanism, while autoregressive next-byte prediction serves as a verification step. We refer to the inference procedure that employs diffusion and verification as **BLT-DV (BLT Diffusion+Verification)**. After generating a block of bytes via diffusion, BLT-DV performs a full forward pass through \mathcal{E} , \mathcal{G} , and \mathcal{D} with a causal mask to produce next-byte predictions. The model then verifies the block diffusion draft with the next-byte predictions using the same procedure as in [Algorithm 2](#).

Importantly, the same model parameters are used for both drafting and verification. The choice of block size B and unmasking strategy determines the balance between generation speed and verification acceptance rate. Empirically, we found that combining one-step diffusion with verification yields the fastest inference. While one-step diffusion alone typically leads to rapid degradation in generation quality, the verification step effectively prevents this issue.

5.3 Evaluating Extensions on Generation Tasks

In [Figure 7](#), we compare 3B-parameter BLT and BLT-D models, along with their respective versions incorporating our new inference extensions. This analysis examines decoder NFEs, encoder/global NFEs, memory bandwidth, and task performance on the same generation tasks described in [Section 4.2](#). [Section B](#) and [Section C](#) also include additional inference hyperparameter sweeps and generation settings for all 1B and 3B model variants of BLT-S and BLT-DV, along with their verification acceptance rates. Overall, all BLT-D and BLT-DV outperform BLT and BLT-S in terms of decoder NFEs. Notably, BLT-DV achieves slightly higher task performance than BLT-D without verification; however, this comes at the cost of increased encoder/global NFEs and thus memory bandwidth due to additional verification calls. BLT-S increases decoder NFEs when compared to BLT, but notably reduces encoder/global NFEs, resulting in improved efficiency and very competitive task performance. Despite these gains, BLT-D-8 and BLT-D-16 (without verification) remain the fastest models, though their task performance is somewhat diminished.

These results suggest several directions for future work. Our experiments used a relatively small decoder; scaling it up could further improve BLT-D/BLT-DV efficiency, since these methods reduce decoder NFEs

Table 1 Performance comparison of 3B-parameter BLT and BLT-D models (block sizes: 4, 8, 16) across five benchmarks. While BLT-D variants exhibit a performance hit due to balancing next-byte prediction with the diffusion objective, the diffusion mechanism enables much faster inference for BLT-D.

Benchmark	BLT 3B	BLT-D-4 3B	BLT-D-8 3B	BLT-D-16 3B
ARC-Easy	74.33	72.39	70.95	66.89
ARC-Challenge	45.75	41.46	41.03	40.43
PIQA	79.38	79.60	78.02	76.93
HellaSwag	74.98	71.86	70.56	69.12
MMLU	41.15	39.07	38.29	37.08

by design. In contrast, with a lightweight decoder, BLT-S’s extra decoder NFEs impose a smaller overhead, making this approach more appealing. Finally, BLT-DV’s verification may be improved by reweighting the training objective—for example, placing greater emphasis on next-byte prediction (used for verification) relative to diffusion.

5.4 Likelihood-based Evaluations

In addition to generation tasks, we further evaluate BLT-D’s verification ability on likelihood-based tasks. Since our diffusion models are also trained with a next-byte prediction objective, they inherently possess the ability to compute likelihoods for sequences. By applying a causal mask to the decoder, we can directly obtain these likelihood estimates. Importantly, this serves as a direct proxy for the quality of BLT-DV’s verification mechanism, which uses the same masking patterns. We benchmark the performance of BLT and BLT-D models across five standard datasets: ARC-Easy (Clark et al., 2018), ARC-Challenge (Clark et al., 2018), PIQA (Bisk et al., 2019), HellaSwag (Zellers et al., 2019), and MMLU (Hendrycks et al., 2021) (see Table 1). The results show that BLT-D variants achieve scores approaching those of the BLT baseline, despite the added complexity of balancing next-byte prediction with the diffusion objective. This demonstrates that BLT-D’s autoregressive capabilities remain robust and that the integration of block diffusion does not compromise autoregressive performance on established language understanding and reasoning tasks. Overall, these findings suggest that BLT-D models can effectively combine block diffusion and next-byte prediction objectives, maintaining strong performance while ensuring high-quality generations.

6 BLT-D Generation Analysis

In this section, we analyze the diversity and efficiency of unconditional generations produced by BLT-D models using entropy-bounded sampling as the unmasking strategy. Because entropy-bounded sampling can be combined with top- p sampling, this setup allows us to sample diverse outputs while varying the amount of parallelism during block diffusion decoding. This analysis focuses on the block generation ability of BLT-D without autoregressive next-byte verification. For each model and sampling configuration, we generate text unconditionally from the start-of-sequence token until reaching a maximum length of 1k bytes.

To quantify diversity, we compute the word-level type-token ratio (TTR) of the generated text after whitespace tokenization, and compare it against the number of decoder network function evaluations (NFEs) required under varying entropy-bounded sampling thresholds (γ) and top- p values. TTR serves as a simple proxy for lexical diversity, with higher values indicating a greater variety of unique words relative to the total word count. The resulting diversity–efficiency trade-off is shown in Figure 8.

Our results show a clear trend: as the number of decoder calls increases, the type-token ratio also increases. This suggests that more decoder forward passes are associated with the generation of more diverse text. Conversely, when the model produces repetitive or highly predictable text, it requires fewer decoder calls, reflecting the lower uncertainty and entropy in those outputs. This relationship highlights a key advantage of block diffusion decoding: it provides a mechanism to explore the trade-off between generation diversity and computational efficiency.

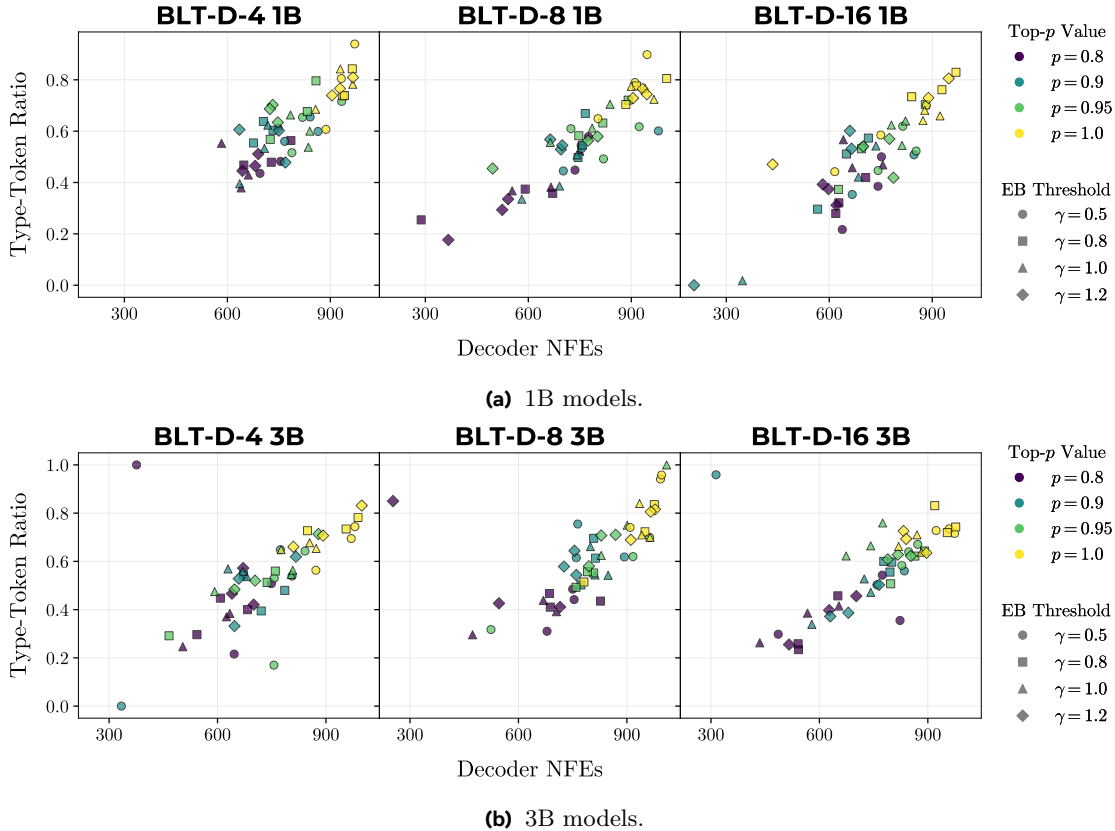


Figure 8 Type-token ratio increases with the number of decoder calls when generating text with BLT-D using entropy-bounded sampling with top- p sampling. This indicates that more decoder passes yield greater diversity, while fewer passes correspond to more repetitive, predictable text. Block diffusion decoding enables exploration of this trade-off between generation diversity and computational efficiency.

7 Conclusion

In this paper, we introduced **BLT Diffusion (BLT-D)**, a byte-level language model that combines BLT’s hierarchical latent tokenization with a block-wise diffusion objective to accelerate generation. BLT-D’s new semi-autoregressive decoder design enables multiple future bytes to be generated in parallel, all while preserving BLT’s dynamic patching and latent token representations. We also proposed two speculative-decoding-inspired extensions: **BLT Self-speculation (BLT-S)**, which uses BLT’s own decoder to draft beyond normal patch boundaries before verification, and **BLT Diffusion+Verification (BLT-DV)**, which verifies diffusion drafts using autoregressive next-byte prediction. Each of these methods substantially reduces total model calls, narrowing the inference-efficiency gap between byte-level and subword-level models.

Limitations and Future Work Here, we note our limitations and point out exciting avenues for future work. The main limitation of our evaluation is that we use network function evaluations (NFEs) and estimated memory bandwidth as proxy metrics for inference efficiency. NFEs are commonly reported in the discrete diffusion literature (see Lou et al. 2024; Arriola et al. 2025) because they isolate algorithmic efficiency from implementation-specific factors such as kernels, hardware utilization, batching strategy, and KV-cache management. Benchmarking BLT, BLT-D, BLT-S, and BLT-DV in a highly optimized inference implementation is therefore an important direction for future work. Other promising directions include experimenting with different patch sizes, tuning the balance between BLT-D’s diffusion and next-byte prediction objectives, scaling training further—which may especially benefit diffusion language models (Ni et al., 2025)—and studying how decoder parameter allocation affects the performance and efficiency of each BLT variant.

References

- Orevaoghene Ahia, Sachin Kumar, Hila Gonen, Jungo Kasai, David Mortensen, Noah Smith, and Yulia Tsvetkov. Do all languages cost the same? Tokenization in the era of commercial language models. In Houda Bouamor, Juan Pino, and Kalika Bali, editors, *Proceedings of the 2023 Conference on Empirical Methods in Natural Language Processing*, pages 9904–9923, Singapore, December 2023. Association for Computational Linguistics. doi: 10.18653/v1/2023.emnlp-main.614. <https://aclanthology.org/2023.emnlp-main.614>.
- Marianne Arriola, Subham Sekhar Sahoo, Aaron Gokaslan, Zhihan Yang, Zhixuan Qi, Jiaqi Han, Justin T Chiu, and Volodymyr Kuleshov. Block diffusion: Interpolating between autoregressive and diffusion language models. In *The Thirteenth International Conference on Learning Representations*, 2025. <https://openreview.net/forum?id=tyEyYT267x>.
- Jacob Austin, Daniel D. Johnson, Jonathan Ho, Daniel Tarlow, and Rianne van den Berg. Structured denoising diffusion models in discrete state-spaces. In M. Ranzato, A. Beygelzimer, Y. Dauphin, P.S. Liang, and J. Wortman Vaughan, editors, *Advances in Neural Information Processing Systems*, volume 34, pages 17981–17993. Curran Associates, Inc., 2021a. https://proceedings.neurips.cc/paper_files/paper/2021/file/958c530554f78bcd8e97125b70e6973d-Paper.pdf.
- Jacob Austin, Augustus Odena, Maxwell Nye, Maarten Bosma, Henryk Michalewski, David Dohan, Ellen Jiang, Carrie Cai, Michael Terry, Quoc Le, and Charles Sutton. Program synthesis with large language models. *arXiv preprint arXiv: 2108.07732*, 2021b. <https://arxiv.org/abs/2108.07732>.
- Heli Ben-Hamu, Itai Gat, Daniel Severo, Niklas Nolte, and Brian Karrer. Accelerated sampling from masked diffusion models via entropy bounded unmasking. In *The Thirty-ninth Annual Conference on Neural Information Processing Systems*, 2025. <https://openreview.net/forum?id=WBCbHT1NKO>.
- Yonatan Bisk, Rowan Zellers, Ronan Le Bras, Jianfeng Gao, and Yejin Choi. Piqa: Reasoning about physical commonsense in natural language. *arXiv preprint arXiv: 1911.11641*, 2019. <https://arxiv.org/abs/1911.11641>.
- Tianle Cai, Yuhong Li, Zhengyang Geng, Hongwu Peng, Jason D. Lee, Deming Chen, and Tri Dao. Medusa: Simple llm inference acceleration framework with multiple decoding heads. In *Proceedings of the 41st International Conference on Machine Learning*, ICML’24. JMLR.org, 2024.
- Andrew Campbell, Joe Benton, Valentin De Bortoli, Thomas Rainforth, George Deligiannidis, and Arnaud Doucet. A continuous time framework for discrete denoising models. In S. Koyejo, S. Mohamed, A. Agarwal, D. Belgrave, K. Cho, and A. Oh, editors, *Advances in Neural Information Processing Systems*, volume 35, pages 28266–28279. Curran Associates, Inc., 2022. https://proceedings.neurips.cc/paper_files/paper/2022/file/b5b528767aa35f5b1a60fe0aaeca0563-Paper-Conference.pdf.
- Mark Chen, Jerry Tworek, Heewoo Jun, Qiming Yuan, Henrique Ponde de Oliveira Pinto, Jared Kaplan, Harri Edwards, Yuri Burda, Nicholas Joseph, Greg Brockman, Alex Ray, Raul Puri, Gretchen Krueger, Michael Petrov, Heidy Khlaaf, Girish Sastry, Pamela Mishkin, Brooke Chan, Scott Gray, Nick Ryder, Mikhail Pavlov, Alethea Power, Lukasz Kaiser, Mohammad Bavarian, Clemens Winter, Philippe Tillet, Felipe Petroski Such, Dave Cummings, Matthias Plappert, Fotios Chantzis, Elizabeth Barnes, Ariel Herbert-Voss, William Hebgen Guss, Alex Nichol, Alex Paino, Nikolas Tezak, Jie Tang, Igor Babuschkin, Suchir Balaji, Shantanu Jain, William Saunders, Christopher Hesse, Andrew N. Carr, Jan Leike, Josh Achiam, Vedant Misra, Evan Morikawa, Alec Radford, Matthew Knight, Miles Brundage, Mira Murati, Katie Mayer, Peter Welinder, Bob McGrew, Dario Amodei, Sam McCandlish, Ilya Sutskever, and Wojciech Zaremba. Evaluating large language models trained on code. *arXiv preprint arXiv: 2107.03374*, 2021. <https://arxiv.org/abs/2107.03374>.
- Jonathan H. Clark, Dan Garrette, Iulia Turc, and John Wieting. CANINE: Pre-training an efficient tokenization-free encoder for language representation. *Transactions of the Association for Computational Linguistics*, 10:73–91, 2022. doi: 10.1162/tacl_a_00448. <https://aclanthology.org/2022.tacl-1.5>.
- Peter Clark, Isaac Cowhey, Oren Etzioni, Tushar Khot, Ashish Sabharwal, Carissa Schoenick, and Oyvind Tafjord. Think you have solved question answering? try arc, the ai2 reasoning challenge. *arXiv preprint arXiv: 1803.05457*, 2018. <https://arxiv.org/abs/1803.05457>.
- Gautier Dagan, Gabriel Synnaeve, and Baptiste Rozière. Getting the most out of your tokenizer for pre-training and domain adaptation. In *Proceedings of the 41st International Conference on Machine Learning*, ICML’24. JMLR.org, 2024.
- Tri Dao, Daniel Y Fu, Stefano Ermon, Atri Rudra, and Christopher Re. Flashattention: Fast and memory-efficient

- exact attention with IO-awareness. In Alice H. Oh, Alekh Agarwal, Danielle Belgrave, and Kyunghyun Cho, editors, *Advances in Neural Information Processing Systems*, 2022. <https://openreview.net/forum?id=H4DqfPSibmx>.
- Jacob Devlin, Ming-Wei Chang, Kenton Lee, and Kristina Toutanova. BERT: Pre-training of deep bidirectional transformers for language understanding. In Jill Burstein, Christy Doran, and Thamar Solorio, editors, *Proceedings of the 2019 Conference of the North American Chapter of the Association for Computational Linguistics: Human Language Technologies, Volume 1 (Long and Short Papers)*, pages 4171–4186, Minneapolis, Minnesota, June 2019. Association for Computational Linguistics. doi: 10.18653/v1/N19-1423. <https://aclanthology.org/N19-1423/>.
- Juechu Dong, BOYUAN FENG, Driss Guessous, Yanbo Liang, and Horace He. Flexattention: A programming model for generating fused attention variants. In *Eighth Conference on Machine Learning and Systems*, 2025. <https://openreview.net/forum?id=2QMYV4bA0R>.
- Lukas Edman, Helmut Schmid, and Alexander Fraser. CUTE: Measuring LLMs’ understanding of their tokens. In Yaser Al-Onaizan, Mohit Bansal, and Yun-Nung Chen, editors, *Proceedings of the 2024 Conference on Empirical Methods in Natural Language Processing*, pages 3017–3026, Miami, Florida, USA, November 2024. Association for Computational Linguistics. doi: 10.18653/v1/2024.emnlp-main.177. <https://aclanthology.org/2024.emnlp-main.177/>.
- Hicham El Boukkouri, Olivier Ferret, Thomas Lavergne, Hiroshi Noji, Pierre Zweigenbaum, and Jun’ichi Tsujii. CharacterBERT: Reconciling ELMo and BERT for word-level open-vocabulary representations from characters. In Donia Scott, Nuria Bel, and Chengqing Zong, editors, *Proceedings of the 28th International Conference on Computational Linguistics*, pages 6903–6915, Barcelona, Spain (Online), December 2020. International Committee on Computational Linguistics. doi: 10.18653/v1/2020.coling-main.609. <https://aclanthology.org/2020.coling-main.609/>.
- Itai Gat, Heli Ben-Hamu, Marton Havasi, Daniel Haziza, Jeremy Reizenstein, Gabriel Synnaeve, David Lopez-Paz, Brian Karrer, and Yaron Lipman. Set block decoding is a language model inference accelerator. *arXiv preprint arXiv: 2509.04185*, 2025. <https://arxiv.org/abs/2509.04185>.
- Marjan Ghazvininejad, Omer Levy, Yinhan Liu, and Luke Zettlemoyer. Mask-predict: Parallel decoding of conditional masked language models. In Kentaro Inui, Jing Jiang, Vincent Ng, and Xiaojun Wan, editors, *Proceedings of the 2019 Conference on Empirical Methods in Natural Language Processing and the 9th International Joint Conference on Natural Language Processing (EMNLP-IJCNLP)*, pages 6112–6121, Hong Kong, China, November 2019. Association for Computational Linguistics. doi: 10.18653/v1/D19-1633. <https://aclanthology.org/D19-1633/>.
- Shansan Gong, Shivam Agarwal, Yizhe Zhang, Jiacheng Ye, Lin Zheng, Mukai Li, Chenxin An, Peilin Zhao, Wei Bi, Jiawei Han, Hao Peng, and Lingpeng Kong. Scaling diffusion language models via adaptation from autoregressive models. In *The Thirteenth International Conference on Learning Representations*, 2025. <https://openreview.net/forum?id=j1tSLYKwg8>.
- Naman Goyal, Cynthia Gao, Vishrav Chaudhary, Peng-Jen Chen, Guillaume Wenzek, Da Ju, Sanjana Krishnan, Marc’Aurelio Ranzato, Francisco Guzmán, and Angela Fan. The Flores-101 evaluation benchmark for low-resource and multilingual machine translation. *Transactions of the Association for Computational Linguistics*, 10:522–538, 2022. doi: 10.1162/tacl_a_00474. <https://aclanthology.org/2022.tacl-1.30/>.
- Ishaan Gulrajani and Tatsunori Hashimoto. Likelihood-based diffusion language models. In *Thirty-seventh Conference on Neural Information Processing Systems*, 2023. <https://openreview.net/forum?id=e2MCL6hObn>.
- Dan Hendrycks, Collin Burns, Steven Basart, Andy Zou, Mantas Mazeika, Dawn Song, and Jacob Steinhardt. Measuring massive multitask language understanding. In *International Conference on Learning Representations*, 2021. <https://openreview.net/forum?id=d7KBjml3GmQ>.
- Jing Huang, Zhengxuan Wu, Kyle Mahowald, and Christopher Potts. Inducing character-level structure in subword-based language models with type-level interchange intervention training. In Anna Rogers, Jordan Boyd-Graber, and Naoaki Okazaki, editors, *Findings of the Association for Computational Linguistics: ACL 2023*, pages 12163–12180, Toronto, Canada, July 2023. Association for Computational Linguistics. doi: 10.18653/v1/2023.findings-acl.770. <https://aclanthology.org/2023.findings-acl.770>.
- Sukjun Hwang, Brandon Wang, and Albert Gu. Dynamic chunking for end-to-end hierarchical sequence modeling. *arXiv preprint arXiv: 2507.07955*, 2025. <https://arxiv.org/abs/2507.07955>.
- Julie Kallini, Shikhar Murty, Christopher D Manning, Christopher Potts, and Róbert Csordás. Mrt5: Dynamic token merging for efficient byte-level language models. In *The Thirteenth International Conference on Learning Representations*, 2025. <https://openreview.net/forum?id=VYWBMq1L7H>.

- Ayush Kaushal and Kyle Mahowald. What do tokens know about their characters and how do they know it? In Marine Carpuat, Marie-Catherine de Marneffe, and Ivan Vladimir Meza Ruiz, editors, *Proceedings of the 2022 Conference of the North American Chapter of the Association for Computational Linguistics: Human Language Technologies*, pages 2487–2507, Seattle, United States, July 2022. Association for Computational Linguistics. doi: 10.18653/v1/2022.naacl-main.179. <https://aclanthology.org/2022.naacl-main.179>.
- Woosuk Kwon, Zhuohan Li, Siyuan Zhuang, Ying Sheng, Lianmin Zheng, Cody Hao Yu, Joseph Gonzalez, Hao Zhang, and Ion Stoica. Efficient memory management for large language model serving with pagedattention. In *Proceedings of the 29th Symposium on Operating Systems Principles, SOSP '23*, page 611–626, New York, NY, USA, 2023. Association for Computing Machinery. ISBN 9798400702297. doi: 10.1145/3600006.3613165. <https://doi.org/10.1145/3600006.3613165>.
- Yaniv Leviathan, Matan Kalman, and Yossi Matias. Fast inference from transformers via speculative decoding. In *Proceedings of the 40th International Conference on Machine Learning, ICML'23*. JMLR.org, 2023.
- Jeffrey Li, Alex Fang, Georgios Smyrnis, Maor Ivgi, Matt Jordan, Samir Yitzhak Gadre, Hritik Bansal, Etash Kumar Guha, Sedrick Keh, Kushal Arora, Saurabh Garg, Rui Xin, Niklas Muennighoff, Reinhard Heckel, Jean Mercat, Mayee F Chen, Suchin Gururangan, Mitchell Wortsman, Alon Albalak, Yonatan Bitton, Marianna Nezhurina, Amro Kamal Mohamed Abbas, Cheng-Yu Hsieh, Dhruva Ghosh, Joshua P Gardner, Maciej Kilian, Hanlin Zhang, Rulin Shao, Sarah M Pratt, Sunny Sanyal, Gabriel Ilharco, Giannis Daras, Kalyani Marathe, Aaron Gokaslan, Jieyu Zhang, Khyathi Chandu, Thao Nguyen, Igor Vasiljevic, Sham M. Kakade, Shuran Song, Sujay Sanghavi, Fartash Faghri, Sewoong Oh, Luke Zettlemoyer, Kyle Lo, Alaaeldin El-Nouby, Hadi Pouransari, Alexander T Toshev, Stephanie Wang, Dirk Groeneveld, Luca Soldaini, Pang Wei Koh, Jenia Jitsev, Thomas Kollar, Alex Dimakis, Yair Carmon, Achal Dave, Ludwig Schmidt, and Vaishaal Shankar. Datacomp-LM: In search of the next generation of training sets for language models. In *The Thirty-eight Conference on Neural Information Processing Systems Datasets and Benchmarks Track*, 2024. <https://openreview.net/forum?id=CNWdWn47IE>.
- Xiang Li, John Thickstun, Ishaan Gulrajani, Percy S Liang, and Tatsunori B Hashimoto. Diffusion-lm improves controllable text generation. In S. Koyejo, S. Mohamed, A. Agarwal, D. Belgrave, K. Cho, and A. Oh, editors, *Advances in Neural Information Processing Systems*, volume 35, pages 4328–4343. Curran Associates, Inc., 2022. https://proceedings.neurips.cc/paper_files/paper/2022/file/1be5bc25d50895ee656b8c2d9eb89d6a-Paper-Conference.pdf.
- Davis Liang, Hila Gonen, Yuning Mao, Rui Hou, Naman Goyal, Marjan Ghazvininejad, Luke Zettlemoyer, and Madian Khabsa. XLM-V: Overcoming the vocabulary bottleneck in multilingual masked language models. In Houda Bouamor, Juan Pino, and Kalika Bali, editors, *Proceedings of the 2023 Conference on Empirical Methods in Natural Language Processing*, pages 13142–13152, Singapore, December 2023. Association for Computational Linguistics. doi: 10.18653/v1/2023.emnlp-main.813. <https://aclanthology.org/2023.emnlp-main.813/>.
- Ilya Loshchilov and Frank Hutter. Decoupled weight decay regularization. *arXiv preprint arXiv: 1711.05101*, 2019. <https://arxiv.org/abs/1711.05101>.
- Aaron Lou, Chenlin Meng, and Stefano Ermon. Discrete diffusion modeling by estimating the ratios of the data distribution. In *Proceedings of the 41st International Conference on Machine Learning, ICML'24*. JMLR.org, 2024.
- Piotr Nawrot, Szymon Tworowski, Michał Tyrolski, Lukasz Kaiser, Yuhuai Wu, Christian Szegedy, and Henryk Michalewski. Hierarchical transformers are more efficient language models. In Marine Carpuat, Marie-Catherine de Marneffe, and Ivan Vladimir Meza Ruiz, editors, *Findings of the Association for Computational Linguistics: NAACL 2022*, pages 1559–1571, Seattle, United States, July 2022. Association for Computational Linguistics. doi: 10.18653/v1/2022.findings-naacl.117. <https://aclanthology.org/2022.findings-naacl.117>.
- Piotr Nawrot, Jan Chorowski, Adrian Lancucki, and Edoardo Maria Ponti. Efficient transformers with dynamic token pooling. In Anna Rogers, Jordan Boyd-Graber, and Naoaki Okazaki, editors, *Proceedings of the 61st Annual Meeting of the Association for Computational Linguistics (Volume 1: Long Papers)*, pages 6403–6417, Toronto, Canada, July 2023. Association for Computational Linguistics. doi: 10.18653/v1/2023.acl-long.353. <https://aclanthology.org/2023.acl-long.353>.
- Jinjie Ni, Qian Liu, Longxu Dou, Chao Du, Zili Wang, Hang Yan, Tianyu Pang, and Michael Qizhe Shieh. Diffusion language models are super data learners. *arXiv preprint arXiv: 2511.03276*, 2025. <https://arxiv.org/abs/2511.03276>.
- Shen Nie, Fengqi Zhu, Zebin You, Xiaolu Zhang, Jingyang Ou, Jun Hu, Jun Zhou, Yankai Lin, Ji-Rong Wen, and Chongxuan Li. Large language diffusion models. *arXiv preprint arXiv: 2502.09992*, 2025. <https://arxiv.org/abs/2502.09992>.

- Artidoro Pagnoni, Ramakanth Pasunuru, Pedro Rodriguez, John Nguyen, Benjamin Muller, Margaret Li, Chunting Zhou, Lili Yu, Jason E Weston, Luke Zettlemoyer, Gargi Ghosh, Mike Lewis, Ari Holtzman, and Srini Iyer. Byte latent transformer: Patches scale better than tokens. In Wanxiang Che, Joyce Nabende, Ekaterina Shutova, and Mohammad Taher Pilehvar, editors, *Proceedings of the 63rd Annual Meeting of the Association for Computational Linguistics (Volume 1: Long Papers)*, pages 9238–9258, Vienna, Austria, July 2025. Association for Computational Linguistics. ISBN 979-8-89176-251-0. doi: 10.18653/v1/2025.acl-long.453. <https://aclanthology.org/2025.acl-long.453/>.
- Aleksandar Petrov, Emanuele La Malfa, Philip Torr, and Adel Bibi. Language model tokenizers introduce unfairness between languages. In *Thirty-seventh Conference on Neural Information Processing Systems*, 2023. <https://openreview.net/forum?id=78yDLKi95p>.
- Reiner Pope, Sholto Douglas, Aakanksha Chowdhery, Jacob Devlin, James Bradbury, Jonathan Heek, Kefan Xiao, Shivani Agrawal, and Jeff Dean. Efficiently scaling transformer inference. In D. Song, M. Carbin, and T. Chen, editors, *Proceedings of Machine Learning and Systems*, volume 5, pages 606–624. Curan, 2023. https://proceedings.mlsys.org/paper_files/paper/2023/file/c4be71ab8d24cdfb45e3d06dbfca2780-Paper-mlsys2023.pdf.
- Danish Pruthi, Bhuwan Dhingra, and Zachary C. Lipton. Combating adversarial misspellings with robust word recognition. In Anna Korhonen, David Traum, and Lluís Màrquez, editors, *Proceedings of the 57th Annual Meeting of the Association for Computational Linguistics*, pages 5582–5591, Florence, Italy, July 2019. Association for Computational Linguistics. doi: 10.18653/v1/P19-1561. <https://aclanthology.org/P19-1561/>.
- Subham Sekhar Sahoo, Marianne Arriola, Yair Schiff, Aaron Gokaslan, Edgar Marroquin, Justin T Chiu, Alexander Rush, and Volodymyr Kuleshov. Simple and effective masked diffusion language models. In A. Globerson, L. Mackey, D. Belgrave, A. Fan, U. Paquet, J. Tomczak, and C. Zhang, editors, *Advances in Neural Information Processing Systems*, volume 37, pages 130136–130184. Curran Associates, Inc., 2024. doi: 10.52202/079017-4135. https://proceedings.neurips.cc/paper_files/paper/2024/file/eb0b13cc515724ab8015bc978fdde0ad-Paper-Conference.pdf.
- Noam Shazeer. Glu variants improve transformer. *arXiv preprint arXiv: 2002.05202*, 2020. <https://arxiv.org/abs/2002.05202>.
- Jiaxin Shi, Kehang Han, Zhe Wang, Arnaud Doucet, and Michalis Titsias. Simplified and generalized masked diffusion for discrete data. In A. Globerson, L. Mackey, D. Belgrave, A. Fan, U. Paquet, J. Tomczak, and C. Zhang, editors, *Advances in Neural Information Processing Systems*, volume 37, pages 103131–103167. Curran Associates, Inc., 2024. doi: 10.52202/079017-3277. https://proceedings.neurips.cc/paper_files/paper/2024/file/bad233b9849f019aead5e5cc60cef70f-Paper-Conference.pdf.
- Aaditya K. Singh and DJ Strouse. Tokenization counts: the impact of tokenization on arithmetic in frontier llms. *arXiv preprint arXiv:2402.14903*, 2024. <https://arxiv.org/abs/2402.14903>.
- Kevin Slagle. Spacebyte: Towards deleting tokenization from large language modeling. *arXiv preprint arXiv:2404.14408*, 2024. <https://arxiv.org/abs/2404.14408>.
- Jianlin Su, Yu Lu, Shengfeng Pan, Ahmed Murtadha, Bo Wen, and Yunfeng Liu. Roformer: Enhanced transformer with rotary position embedding. *arXiv preprint arXiv: 2104.09864*, 2023. <https://arxiv.org/abs/2104.09864>.
- Lichao Sun, Kazuma Hashimoto, Wenpeng Yin, Akari Asai, Jia Li, Philip Yu, and Caiming Xiong. Adv-bert: Bert is not robust on misspellings! generating nature adversarial samples on bert. *arXiv preprint arXiv: 2003.04985*, 2020. <https://arxiv.org/abs/2003.04985>.
- Yi Tay, Vinh Q. Tran, Sebastian Ruder, Jai Gupta, Hyung Won Chung, Dara Bahri, Zhen Qin, Simon Baumgartner, Cong Yu, and Donald Metzler. Charformer: Fast character transformers via gradient-based subword tokenization. In *International Conference on Learning Representations*, 2022. <https://openreview.net/forum?id=JtBRnrIOEFN>.
- Junxiong Wang, Tushaar Gangavarapu, Jing Nathan Yan, and Alexander M Rush. Mambabyte: Token-free selective state space model. In *First Conference on Language Modeling*, 2024. <https://openreview.net/forum?id=X1xNsuKssb>.
- Chengyue Wu, Hao Zhang, Shuchen Xue, Zhijian Liu, Shizhe Diao, Ligeng Zhu, Ping Luo, Song Han, and Enze Xie. Fast-dllm: Training-free acceleration of diffusion llm by enabling kv cache and parallel decoding. *arXiv preprint arXiv: 2505.22618*, 2025. <https://arxiv.org/abs/2505.22618>.
- Wenhan Xiong, Jingyu Liu, Igor Molybog, Hejia Zhang, Prajjwal Bhargava, Rui Hou, Louis Martin, Rashi Rungta, Karthik Abinav Sankararaman, Barlas Oguz, Madian Khabza, Han Fang, Yashar Mehdad, Sharan Narang, Kshitiz Malik, Angela Fan, Shruti Bhosale, Sergey Edunov, Mike Lewis, Sinong Wang, and Hao Ma. Effective long-context scaling of foundation models. In Kevin Duh, Helena Gomez, and Steven Bethard, editors, *Proceedings of*

- the 2024 Conference of the North American Chapter of the Association for Computational Linguistics: Human Language Technologies (Volume 1: Long Papers), pages 4643–4663, Mexico City, Mexico, June 2024. Association for Computational Linguistics. doi: 10.18653/v1/2024.naacl-long.260. <https://aclanthology.org/2024.naacl-long.260/>.
- Linting Xue, Aditya Barua, Noah Constant, Rami Al-Rfou, Sharan Narang, Mihir Kale, Adam Roberts, and Colin Raffel. ByT5: Towards a token-free future with pre-trained byte-to-byte models. *Transactions of the Association for Computational Linguistics*, 10:291–306, 2022. doi: 10.1162/tacl_a_00461. <https://aclanthology.org/2022.tacl-1.17>.
- Jiacheng Ye, Zhihui Xie, Lin Zheng, Jiahui Gao, Zirui Wu, Xin Jiang, Zhenguo Li, and Lingpeng Kong. Dream 7b: Diffusion large language models. *arXiv preprint arXiv: 2508.15487*, 2025. <https://arxiv.org/abs/2508.15487>.
- Lili Yu, Daniel Simig, Colin Flaherty, Armen Aghajanyan, Luke Zettlemoyer, and Mike Lewis. MEGABYTE: Predicting million-byte sequences with multiscale transformers. In *Thirty-seventh Conference on Neural Information Processing Systems*, 2023. <https://openreview.net/forum?id=JTmO2V9Xpz>.
- Zhihang Yuan, Yuzhang Shang, Yang Zhou, Zhen Dong, Zhe Zhou, Chenhao Xue, Bingzhe Wu, Zhikai Li, Qingyi Gu, Yong Jae Lee, Yan Yan, Beidi Chen, Guangyu Sun, and Kurt Keutzer. Llm inference unveiled: Survey and roofline model insights. *arXiv preprint arXiv: 2402.16363*, 2024. <https://arxiv.org/abs/2402.16363>.
- Rowan Zellers, Ari Holtzman, Yonatan Bisk, Ali Farhadi, and Yejin Choi. HellaSwag: Can a machine really finish your sentence? In Anna Korhonen, David Traum, and Lluís Màrquez, editors, *Proceedings of the 57th Annual Meeting of the Association for Computational Linguistics*, pages 4791–4800, Florence, Italy, July 2019. Association for Computational Linguistics. doi: 10.18653/v1/P19-1472. <https://aclanthology.org/P19-1472/>.
- Biao Zhang and Rico Sennrich. Root mean square layer normalization. In H. Wallach, H. Larochelle, A. Beygelzimer, F. d'Alché-Buc, E. Fox, and R. Garnett, editors, *Advances in Neural Information Processing Systems*, volume 32. Curran Associates, Inc., 2019. https://proceedings.neurips.cc/paper_files/paper/2019/file/1e8a19426224ca89e83cef47f1e7f53b-Paper.pdf.
- Jun Zhang, Jue Wang, Huan Li, Lidan Shou, Ke Chen, Gang Chen, and Sharad Mehrotra. Draft & verify: Lossless large language model acceleration via self-speculative decoding. In Lun-Wei Ku, Andre Martins, and Vivek Srikumar, editors, *Proceedings of the 62nd Annual Meeting of the Association for Computational Linguistics (Volume 1: Long Papers)*, pages 11263–11282, Bangkok, Thailand, August 2024. Association for Computational Linguistics. doi: 10.18653/v1/2024.acl-long.607. <https://aclanthology.org/2024.acl-long.607/>.
- Lin Zheng, Xueliang Zhao, Guangtao Wang, Chen Wu, David Dong, Angela Wang, Mingran Wang, Yun Du, Haige Bo, Amol Sharma, Bo Li, Kejie Zhang, Changran Hu, Urmish Thakker, and Lingpeng Kong. Evabyte: Efficient byte-level language models at scale, 2025. <https://hkunlp.github.io/blog/2025/evabyte>.
- Zhejian Zhou, Jiayu Wang, Dahua Lin, and Kai Chen. Scaling behavior for large language models regarding numeral systems: An example using pythia. In Yaser Al-Onaizan, Mohit Bansal, and Yun-Nung Chen, editors, *Findings of the Association for Computational Linguistics: EMNLP 2024*, pages 3806–3820, Miami, Florida, USA, November 2024. Association for Computational Linguistics. doi: 10.18653/v1/2024.findings-emnlp.218. <https://aclanthology.org/2024.findings-emnlp.218/>.

Appendix

A Architecture and Optimization Details

A.1 Architecture Implementation Details

For all the BLT and BLT-D models we train, we maintain the same Transformer implementation details from the original BLT: the feed-forward layers use the SwiGLU activation function (Shazeer, 2020), all self-attention modules use rotary positional embeddings (RoPE, Su et al. 2023) with $\theta = 500000$ (Xiong et al., 2024), and layer normalization is done with RMSNorm (Zhang and Sennrich, 2019).

For self-attention in the encoder and global model, where the mask is fixed and follows a standard causal pattern with a fixed window, we use FlashAttention (Dao et al., 2022) with a window size of 512. For all cross-attention modules and the decoder’s self-attention module, which requires carefully constructed custom masks that depend on the patch structure and vary per example, we use FlexAttention (Dong et al., 2025). FlexAttention streamlines the implementation of attention mechanisms with structured sparsity in PyTorch and allows users to define custom attention masks, all while achieving performance levels on par with specialized, manually optimized attention kernels.

A.2 Pre-training Optimization and Hyperparameter Settings

All BLT/BLT-D 1B models are trained for 240,000 steps with a batch size of 2^{19} tokens per step (approximately 2 million bytes), and our 3B models are trained for 480,000 steps with a batch size of 2^{20} tokens per step (approximately 4 million bytes). All models use the AdamW optimizer (Loshchilov and Hutter, 2019) with $\beta_1 = 0.9$, $\beta_2 = 0.95$, and $\epsilon = 10^{-8}$. All models use a cosine learning rate schedule that linearly warms-up to a peak learning rate of 4×10^{-4} and decays to 0. The 1B models warm-up to 2000 steps; the 3B models warm-up to 4000 steps. We apply a weight decay of 0.1, and global gradient clipping at a threshold of 1.0.

B All 1B Model Results

In this section, we report results for all 1B models. Figure 9 and Figure 10 present the 1B counterparts of the generation-task results from Section 4.3 and Section 5.3 for BLT, BLT-D, BLT-S, and BLT-DV. Table 2 reports the likelihood-based evaluation results for the 1B models.

We also run a larger sweep over inference hyperparameters for the 1B models on the generation tasks. For BLT-D, we evaluate confidence-based unmasking with thresholds $\alpha \in \{0.5, 0.7\}$, as well as EB sampling with thresholds $\gamma \in \{0.8, 1.0\}$. For BLT-DV, we use more permissive settings that unmask more bytes per step; i.e., we *decrease* α for confidence-based unmasking or *increase* γ for EB sampling. Specifically, we test $\alpha = 0.3$, $\gamma \in \{1.5, 2.0\}$, and one-step diffusion that unmask all byte positions at once. For BLT-S, we use speculation windows $k \in \{4, 8, 16\}$. For BLT-S and BLT-DV, we also report the verification acceptance rate, defined as the fraction of drafted bytes that are accepted after verification. Table 3, Table 4, Table 5, and Table 6 report results on French-to-English translation, German-to-English translation, HumanEval, and MBPP, respectively.

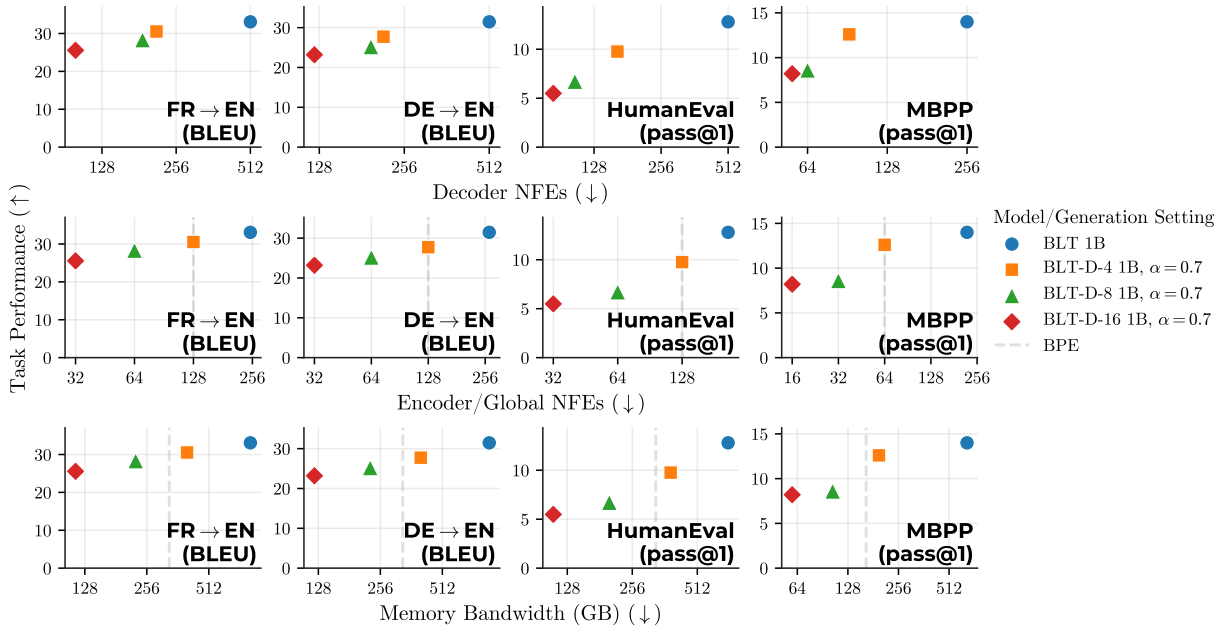


Figure 9 Generation task results of 1B-parameter variants of BLT, BLT-D-4, BLT-D-8, and BLT-D-16. Higher is better for task performance; lower is better for NFEs and memory bandwidth. The NFEs and memory bandwidth for a byte-pair encoding (BPE) model matching BLT’s global model size are shown as a dashed line.

Table 2 Performance comparison of BLT and BLT-D (block sizes 4, 8, 16) at 1B parameters across five benchmarks.

Benchmark	BLT 1B	BLT-D-4 1B	BLT-D-8 1B	BLT-D-16 1B
ARC-Easy	63.21	60.76	61.06	59.83
ARC-Challenge	34.94	32.96	34.16	32.88
PIQA	75.46	74.48	73.56	72.36
HellaSwag	60.17	59.06	58.34	57.13
MMLU	33.90	33.60	32.28	32.09

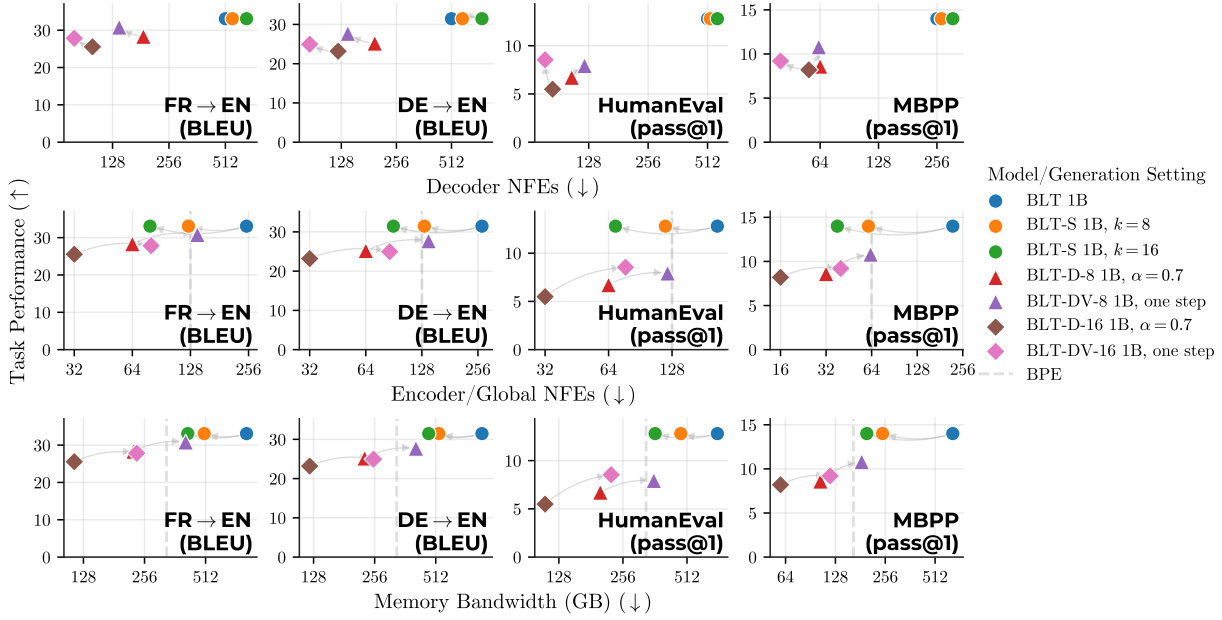


Figure 10 Generation task results for 1B-parameter variants of BLT, BLT-S, BLT-D, and BLT-DV. For space, we report results only for $k \in \{8, 16\}$ and $B \in \{8, 16\}$. Arrows indicate the same model evaluated with different inference methods.

Table 3 Full French-to-English translation results for 1B-parameter models across various generation settings.

Model	Generation Setting	BLEU	Diffusion/Speculation Sampling Strategy	Acceptance Rate (%)	Decoder NFEs	Global NFEs	Memory Bandwidth (GB)	Memory Decrease vs. BLT (%)
BLT 1B	BLT (AR)	33.08	—	—	512	250	814.95	—
	BLT-S (AR+self-speculation)	33.08	$k = 4$	96.77	526	212	719.45	11.72
			$k = 8$	91.14	558	125	504.08	38.15
			$k = 16$	76.93	664	79	418.26	48.68
BLT-D-4 1B	BLT-D (diffusion only)	30.01	Confidence-based, $\alpha = 0.5$	—	184	128	392.17	51.88
		30.53	Confidence-based, $\alpha = 0.7$	—	213	128	401.38	50.75
		30.59	EB sampling, $\gamma = 0.8$	—	261	128	416.32	48.91
		30.68	EB sampling, $\gamma = 1.0$	—	249	128	412.68	49.36
	BLT-DV (diffusion+verification)	32.65	Confidence-based, $\alpha = 0.3$	93.40	239	217	642.00	21.22
BLT-D-8 1B	BLT-D (diffusion only)	26.70	Confidence-based, $\alpha = 0.5$	—	147	64	213.50	73.80
		28.32	Confidence-based, $\alpha = 0.7$	—	187	64	226.00	72.27
		28.11	EB sampling, $\gamma = 0.8$	—	259	64	248.91	69.46
		28.14	EB sampling, $\gamma = 1.0$	—	244	64	243.95	70.07
	BLT-DV (diffusion+verification)	30.80	Confidence-based, $\alpha = 0.3$	83.81	176	134	406.37	50.14
BLT-D-16 1B	BLT-D (diffusion only)	23.68	Confidence-based, $\alpha = 0.5$	—	77	32	107.92	86.76
		25.55	Confidence-based, $\alpha = 0.7$	—	100	32	115.34	85.85
		25.49	EB sampling, $\gamma = 0.8$	—	179	32	140.24	82.79
		25.44	EB sampling, $\gamma = 1.0$	—	167	32	136.42	83.26
	BLT-DV (diffusion+verification)	27.84	Confidence-based, $\alpha = 0.3$	82.49	112	74	230.57	71.71
BLT-DV (diffusion+verification)	EB sampling, $\gamma = 1.5$	86.53	201	71	248.80	69.47		
	EB sampling, $\gamma = 2.0$	86.27	184	71	244.13	70.04		
	one step	77.19	80	80	234.33	71.25		

Table 4 Full **German-to-English** translation results for **1B-parameter** models across various generation settings.

Model	Generation Setting	BLEU	Diffusion/Speculation Sampling Strategy	Acceptance Rate (%)	Decoder NFEs	Global NFEs	Memory Bandwidth (GB)	Memory Decrease vs. BLT (%)
BLT 1B	BLT (AR)	31.46	—	—	512	269	864.76	—
	BLT-S (AR+self-speculation)	31.46	$k = 4$	95.08	534	215	729.53	15.64
			$k = 8$	86.09	587	132	530.01	38.71
			$k = 16$	67.51	751	90	472.52	45.36
BLT-D-4 1B	BLT-D (diffusion only)	27.30	Confidence-based, $\alpha = 0.5$	—	189	128	393.58	54.49
		27.73	Confidence-based, $\alpha = 0.7$	—	216	128	402.31	53.48
		27.85	EB sampling, $\gamma = 0.8$	—	259	128	415.71	51.93
		27.99	EB sampling, $\gamma = 1.0$	—	247	128	411.90	52.37
	BLT-DV (diffusion+verification)	29.56	Confidence-based, $\alpha = 0.3$	93.45	238	217	641.53	25.81
			EB sampling, $\gamma = 1.5$	94.42	284	215	651.55	24.66
			EB sampling, $\gamma = 2.0$	94.33	273	215	648.30	25.03
			one step	93.36	217	217	635.20	26.55
BLT-D-8 1B	BLT-D (diffusion only)	24.20	Confidence-based, $\alpha = 0.5$	—	157	64	216.67	74.94
		25.20	Confidence-based, $\alpha = 0.7$	—	195	64	228.50	73.58
		24.77	EB sampling, $\gamma = 0.8$	—	252	64	246.55	71.49
		24.92	EB sampling, $\gamma = 1.0$	—	238	64	242.16	72.00
	BLT-DV (diffusion+verification)	27.71	Confidence-based, $\alpha = 0.3$	82.94	188	135	414.05	52.12
			EB sampling, $\gamma = 1.5$	85.35	278	132	433.24	49.90
			EB sampling, $\gamma = 2.0$	85.16	260	132	428.32	50.47
			one step	80.41	139	139	408.96	52.71
BLT-D-16 1B	BLT-D (diffusion only)	21.87	Confidence-based, $\alpha = 0.5$	—	94	32	113.32	86.90
		23.19	Confidence-based, $\alpha = 0.7$	—	123	32	122.48	85.84
		22.66	EB sampling, $\gamma = 0.8$	—	208	32	149.20	82.75
		22.66	EB sampling, $\gamma = 1.0$	—	195	32	145.24	83.20
	BLT-DV (diffusion+verification)	24.96	Confidence-based, $\alpha = 0.3$	76.51	144	80	256.03	70.39
			EB sampling, $\gamma = 1.5$	80.15	245	76	278.02	67.85
			EB sampling, $\gamma = 2.0$	79.93	226	77	272.54	68.48
			one step	71.75	86	86	252.74	70.77

Table 5 Full **HumanEval** task results for **1B-parameter** models across various generation settings.

Model	Generation Setting	PASS@1	Diffusion/Speculation Sampling Strategy	Acceptance Rate (%)	Decoder NFEs	Global NFEs	Memory Bandwidth (GB)	Memory Decrease vs. BLT (%)
BLT 1B	BLT (AR)	12.80	—	—	512	210	711.20	—
	BLT-S (AR+self-speculation)	12.80	$k = 4$	98.77	517	208	707.67	0.50
			$k = 8$	96.45	529	119	478.64	32.70
			$k = 16$	88.92	574	69	362.77	48.99
BLT-D-4 1B	BLT-D (diffusion only)	8.54	Confidence-based, $\alpha = 0.5$	—	147	128	380.26	46.53
		9.76	Confidence-based, $\alpha = 0.7$	—	163	128	385.31	45.82
		10.37	EB sampling, $\gamma = 0.8$	—	195	128	395.62	44.37
		10.37	EB sampling, $\gamma = 1.0$	—	185	128	392.50	44.81
	BLT-DV (diffusion+verification)	9.15	Confidence-based, $\alpha = 0.3$	97.76	213	209	613.63	13.72
			EB sampling, $\gamma = 1.5$	98.22	239	208	619.73	12.86
			EB sampling, $\gamma = 2.0$	98.22	231	208	617.23	13.21
			one step	97.69	209	209	612.52	13.88
BLT-D-8 1B	BLT-D (diffusion only)	6.71	Confidence-based, $\alpha = 0.5$	—	87	64	194.69	72.62
		6.71	Confidence-based, $\alpha = 0.7$	—	105	64	200.35	71.83
		7.93	EB sampling, $\gamma = 0.8$	—	155	64	215.99	69.63
		7.93	EB sampling, $\gamma = 1.0$	—	144	64	212.55	70.11
	BLT-DV (diffusion+verification)	7.93	Confidence-based, $\alpha = 0.3$	93.73	131	121	358.72	49.56
			EB sampling, $\gamma = 1.5$	95.25	180	119	369.54	48.04
			EB sampling, $\gamma = 2.0$	95.15	169	119	366.22	48.51
			one step	93.13	122	122	357.62	49.72
BLT-D-16 1B	BLT-D (diffusion only)	3.66	Confidence-based, $\alpha = 0.5$	—	61	32	102.82	85.54
		5.49	Confidence-based, $\alpha = 0.7$	—	84	32	110.27	84.50
		6.10	EB sampling, $\gamma = 0.8$	—	148	32	130.41	81.66
		5.49	EB sampling, $\gamma = 1.0$	—	137	32	126.72	82.18
	BLT-DV (diffusion+verification)	8.54	Confidence-based, $\alpha = 0.3$	81.72	97	74	225.05	68.36
			EB sampling, $\gamma = 1.5$	86.99	180	70	240.02	66.25
			EB sampling, $\gamma = 2.0$	86.75	164	70	235.13	66.94
			one step	78.92	77	77	225.34	68.32

Table 6 Full MBPP task results for **1B-parameter** models across various generation settings.

Model	Generation Setting	PASS@1	Diffusion/Speculation Sampling Strategy	Acceptance Rate (%)	Decoder NFEs	Global NFEs	Memory Bandwidth (GB)	Memory Decrease vs. BLT (%)
BLT 1B	BLT (AR)	14.00	—	—	256	220	654.61	—
	BLT-S (AR+self-speculation)	14.00	$k = 4$	98.02	261	105	358.79	45.19
			$k = 8$	94.54	270	61	246.50	62.34
			$k = 16$	82.43	309	38	198.05	69.75
BLT-D-4 1B	BLT-D (diffusion only)	9.60	Confidence-based, $\alpha = 0.5$	—	79	64	191.88	70.69
		12.60	Confidence-based, $\alpha = 0.7$	—	92	64	195.97	70.06
		12.40	EB sampling, $\gamma = 0.8$	—	110	64	201.84	69.17
		12.00	EB sampling, $\gamma = 1.0$	—	105	64	200.09	69.43
	BLT-DV (diffusion+verification)	13.80	Confidence-based, $\alpha = 0.3$	96.42	109	106	312.00	52.34
			EB sampling, $\gamma = 1.5$	97.30	132	105	317.04	51.57
			EB sampling, $\gamma = 2.0$	97.10	126	105	315.65	51.78
			one step	96.18	106	106	311.33	52.44
BLT-D-8 1B	BLT-D (diffusion only)	6.40	Confidence-based, $\alpha = 0.5$	—	50	32	99.46	84.81
		8.60	Confidence-based, $\alpha = 0.7$	—	64	32	103.89	84.13
		7.60	EB sampling, $\gamma = 0.8$	—	92	32	112.74	82.78
		7.60	EB sampling, $\gamma = 1.0$	—	86	32	110.91	83.06
	BLT-DV (diffusion+verification)	10.80	Confidence-based, $\alpha = 0.3$	91.56	68	62	184.69	71.79
			EB sampling, $\gamma = 1.5$	93.79	103	61	192.32	70.62
			EB sampling, $\gamma = 2.0$	94.00	95	61	189.54	71.05
			one step	90.60	63	63	184.50	71.82
BLT-D-16 1B	BLT-D (diffusion only)	5.60	Confidence-based, $\alpha = 0.5$	—	40	16	54.48	91.68
		8.20	Confidence-based, $\alpha = 0.7$	—	56	16	59.66	90.89
		8.00	EB sampling, $\gamma = 0.8$	—	89	16	69.91	89.32
		8.20	EB sampling, $\gamma = 1.0$	—	82	16	67.74	89.65
	BLT-DV (diffusion+verification)	9.20	Confidence-based, $\alpha = 0.3$	79.32	53	38	117.97	81.98
			EB sampling, $\gamma = 1.5$	86.31	100	35	125.17	80.88
			EB sampling, $\gamma = 2.0$	85.85	91	36	122.99	81.21
			one step	75.34	40	40	119.00	81.82

C All 3B Model Results

In this section, we present the results of a larger sweep over inference hyperparameters for our 3B BLT-D, BLT-DV, and BLT-S models on the generation tasks. For BLT-D, we evaluate confidence-based unmasking with thresholds $\alpha \in \{0.5, 0.7\}$, as well as EB sampling with thresholds $\gamma \in \{0.8, 1.0\}$. For BLT-DV, we use more permissive settings that unmask more bytes per step; i.e., we *decrease* α for confidence-based unmasking or *increase* γ for EB sampling. Specifically, we test $\alpha = 0.3$, $\gamma \in \{1.5, 2.0\}$, and one-step diffusion that unmask all byte positions at once. For BLT-S, we use speculation windows $k \in \{4, 8, 16\}$. For BLT-S and BLT-DV, we also report the verification acceptance rate, defined as the fraction of drafted bytes that are accepted after verification. Table 7, Table 8, Table 9, and Table 10 report results on French-to-English translation, German-to-English translation, HumanEval, and MBPP, respectively.

Table 7 Full **French-to-English** translation results for **3B-parameter** models across various generation settings.

Model	Generation Setting	BLEU	Diffusion/Speculation Sampling Strategy	Acceptance Rate (%)	Decoder NFEs	Global NFEs	Memory Bandwidth (GB)	Memory Decrease vs. BLT (%)
BLT 3B	BLT (AR)	40.72	—	—	512	308	1920.99	—
	BLT-S (AR+self-speculation)	40.72	$k = 4$	94.93	534	215	1395.99	27.33
			$k = 8$	87.16	580	130	928.73	51.65
			$k = 16$	69.93	724	87	727.17	62.15
BLT-D-4 3B	BLT-D (diffusion only)	37.75	Confidence-based, $\alpha = 0.5$	—	185	128	787.36	59.01
		38.09	Confidence-based, $\alpha = 0.7$	—	216	128	797.58	58.48
		37.79	EB sampling, $\gamma = 0.8$	—	261	128	811.75	57.74
		37.83	EB sampling, $\gamma = 1.0$	—	250	128	808.18	57.93
	BLT-DV (diffusion+verification)	38.89	Confidence-based, $\alpha = 0.3$	94.37	236	215	1300.92	32.28
			EB sampling, $\gamma = 1.5$	95.37	290	213	1308.01	31.91
			EB sampling, $\gamma = 2.0$	95.32	277	213	1304.23	32.11
			one step	93.12	217	217	1307.60	31.93
BLT-D-8 3B	BLT-D (diffusion only)	35.94	Confidence-based, $\alpha = 0.5$	—	143	64	409.85	78.66
		37.09	Confidence-based, $\alpha = 0.7$	—	179	64	421.51	78.06
		36.54	EB sampling, $\gamma = 0.8$	—	249	64	443.89	76.89
		36.60	EB sampling, $\gamma = 1.0$	—	235	64	439.56	77.12
	BLT-DV (diffusion+verification)	38.66	Confidence-based, $\alpha = 0.3$	86.25	166	130	797.43	58.49
			EB sampling, $\gamma = 1.5$	89.34	251	126	802.07	58.25
			EB sampling, $\gamma = 2.0$	88.79	236	127	801.11	58.30
			one step	84.63	133	133	799.94	58.36
BLT-D-16 3B	BLT-D (diffusion only)	31.64	Confidence-based, $\alpha = 0.5$	—	123	32	221.58	88.47
		34.05	Confidence-based, $\alpha = 0.7$	—	162	32	233.87	87.83
		33.75	EB sampling, $\gamma = 0.8$	—	242	32	259.55	86.49
		33.69	EB sampling, $\gamma = 1.0$	—	229	32	255.41	86.70
	BLT-DV (diffusion+verification)	35.23	Confidence-based, $\alpha = 0.3$	67.22	179	89	568.61	70.40
			EB sampling, $\gamma = 1.5$	75.09	293	80	553.65	71.18
			EB sampling, $\gamma = 2.0$	74.77	271	81	548.64	71.44
			one step	60.33	99	99	598.66	68.84

Table 8 Full **German-to-English** translation results for **3B-parameter** models across various generation settings.

Model	Generation Setting	BLEU	Diffusion/Speculation Sampling Strategy	Acceptance Rate (%)	Decoder NFEs	Global NFEs	Memory Bandwidth (GB)	Memory Decrease vs. BLT (%)	
BLT 3B	BLT (AR)	38.82	—	—	512	283	1776.54	—	
	BLT-S (AR+self-speculation)	38.82	$k = 4$	95.67	531	214	1387.43	21.90	
			$k = 8$	87.82	576	129	922.56	48.07	
			$k = 16$	70.23	721	86	724.53	59.22	
BLT-D-4 3B	BLT-D (diffusion only)	35.74	Confidence-based, $\alpha = 0.5$	—	186	128	787.95	55.65	
		36.29	Confidence-based, $\alpha = 0.7$	—	214	128	796.70	55.15	
		36.48	EB sampling, $\gamma = 0.8$	—	247	128	807.51	54.55	
		36.53	EB sampling, $\gamma = 1.0$	—	237	128	804.01	54.74	
	BLT-DV (diffusion+verification)	37.46	Confidence-based, $\alpha = 0.3$	94.35	235	215	1300.96	26.77	
			EB sampling, $\gamma = 1.5$	95.08	279	214	1307.33	26.41	
BLT-D-8 3B	BLT-D (diffusion only)	33.83	Confidence-based, $\alpha = 0.5$	—	146	64	411.05	76.86	
		35.29	Confidence-based, $\alpha = 0.7$	—	180	64	421.74	76.26	
		35.41	EB sampling, $\gamma = 0.8$	—	230	64	437.95	75.35	
		35.46	EB sampling, $\gamma = 1.0$	—	217	64	433.80	75.58	
	BLT-DV (diffusion+verification)	37.11	Confidence-based, $\alpha = 0.3$	84.56	183	133	817.54	53.98	
			EB sampling, $\gamma = 1.5$	86.52	264	130	827.75	53.41	
			EB sampling, $\gamma = 2.0$	86.37	249	130	824.42	53.59	
	BLT-D-16 3B	BLT-D (diffusion only)	30.30	Confidence-based, $\alpha = 0.5$	—	109	32	217.12	87.78
			32.62	Confidence-based, $\alpha = 0.7$	—	136	32	225.81	87.29
			32.56	EB sampling, $\gamma = 0.8$	—	206	32	247.99	86.04
32.48			EB sampling, $\gamma = 1.0$	—	191	32	243.35	86.30	
BLT-DV (diffusion+verification)		34.52	Confidence-based, $\alpha = 0.3$	74.49	161	83	524.04	70.50	
			EB sampling, $\gamma = 1.5$	77.89	263	79	534.83	69.89	
		EB sampling, $\gamma = 2.0$	77.66	245	79	530.54	70.14		
		one step	70.44	88	88	529.76	70.18		

Table 9 Full **HumanEval** task results for **3B-parameter** models across various generation settings.

Model	Generation Setting	PASS@1	Diffusion/Speculation Sampling Strategy	Acceptance Rate (%)	Decoder NFEs	Global NFEs	Memory Bandwidth (GB)	Memory Decrease vs. BLT (%)
BLT 3B	BLT (AR)	22.56	—	—	512	250	1590.45	—
	BLT-S (AR+self-speculation)	22.56	$k = 4$	98.68	518	208	1353.39	14.91
			$k = 8$	95.96	532	120	853.11	46.36
			$k = 16$	88.01	581	70	585.81	63.17
BLT-D-4 3B	BLT-D (diffusion only)	17.07	Confidence-based, $\alpha = 0.5$	—	144	128	774.41	51.31
		18.90	Confidence-based, $\alpha = 0.7$	—	159	128	779.20	51.01
		18.90	EB sampling, $\gamma = 0.8$	—	188	128	788.50	50.42
		18.90	EB sampling, $\gamma = 1.0$	—	180	128	785.82	50.59
	BLT-DV (diffusion+verification)	18.90	Confidence-based, $\alpha = 0.3$	97.97	214	208	1257.30	20.95
			EB sampling, $\gamma = 1.5$	98.29	239	208	1262.78	20.60
			EB sampling, $\gamma = 2.0$	98.26	232	208	1260.65	20.74
			one step	97.74	209	209	1258.33	20.88
BLT-D-8 3B	BLT-D (diffusion only)	10.37	Confidence-based, $\alpha = 0.5$	—	88	64	392.51	75.32
		15.85	Confidence-based, $\alpha = 0.7$	—	106	64	398.04	74.97
		15.24	EB sampling, $\gamma = 0.8$	—	152	64	412.75	74.05
		15.24	EB sampling, $\gamma = 1.0$	—	142	64	409.53	74.25
	BLT-DV (diffusion+verification)	16.46	Confidence-based, $\alpha = 0.3$	94.51	130	120	728.09	54.22
			EB sampling, $\gamma = 1.5$	96.04	176	118	733.00	53.91
			EB sampling, $\gamma = 2.0$	95.91	165	119	730.33	54.08
			one step	93.63	121	121	731.02	54.04
BLT-D-16 3B	BLT-D (diffusion only)	8.54	Confidence-based, $\alpha = 0.5$	—	62	32	201.98	87.30
		9.76	Confidence-based, $\alpha = 0.7$	—	84	32	208.94	86.86
		11.59	EB sampling, $\gamma = 0.8$	—	143	32	227.97	85.67
		10.98	EB sampling, $\gamma = 1.0$	—	133	32	224.65	85.88
	BLT-DV (diffusion+verification)	14.02	Confidence-based, $\alpha = 0.3$	83.61	94	72	445.22	72.01
			EB sampling, $\gamma = 1.5$	87.77	172	69	449.96	71.71
			EB sampling, $\gamma = 2.0$	87.61	155	69	445.39	72.00
			one step	80.68	75	75	453.15	71.51

Table 10 Full MBPP task results for **3B-parameter** models across various generation settings.

Model	Generation Setting	PASS@1	Diffusion/Speculation Sampling Strategy	Acceptance Rate (%)	Decoder NFEs	Global NFEs	Memory Bandwidth (GB)	Memory Decrease vs. BLT (%)
BLT 3B	BLT (AR)	29.60	—	—	256	222	1349.34	—
	BLT-S (AR+self-speculation)	29.60	$k = 4$	98.21	260	105	685.35	49.21
			$k = 8$	94.84	269	61	436.89	67.62
$k = 16$			84.41	302	37	310.63	76.98	
BLT-D-4 3B	BLT-D (diffusion only)	24.60	Confidence-based, $\alpha = 0.5$	—	76	64	388.71	71.19
		26.00	Confidence-based, $\alpha = 0.7$	—	89	64	392.59	70.90
		25.80	EB sampling, $\gamma = 0.8$	—	107	64	398.39	70.48
		25.80	EB sampling, $\gamma = 1.0$	—	101	64	396.72	70.60
	BLT-DV (diffusion+verification)	27.20	EB sampling, $\gamma = 1.5$	97.94	129	105	639.19	52.63
			EB sampling, $\gamma = 2.0$	97.86	123	105	637.77	52.74
			one step	96.98	105	105	635.95	52.87
BLT-D-8 3B	BLT-D (diffusion only)	18.40	Confidence-based, $\alpha = 0.5$	—	49	32	197.75	85.34
		20.80	Confidence-based, $\alpha = 0.7$	—	63	32	202.22	85.01
		23.20	EB sampling, $\gamma = 0.8$	—	88	32	210.29	84.42
		22.40	EB sampling, $\gamma = 1.0$	—	82	32	208.37	84.56
	BLT-DV (diffusion+verification)	27.00	Confidence-based, $\alpha = 0.3$	92.68	67	61	373.68	72.31
			EB sampling, $\gamma = 1.5$	94.85	99	60	376.71	72.08
			EB sampling, $\gamma = 2.0$	94.65	92	60	375.13	72.20
			one step	91.87	62	62	374.64	72.24
BLT-D-16 3B	BLT-D (diffusion only)	10.60	Confidence-based, $\alpha = 0.5$	—	39	16	103.64	92.32
		15.80	Confidence-based, $\alpha = 0.7$	—	55	16	108.78	91.94
		15.60	EB sampling, $\gamma = 0.8$	—	88	16	119.48	91.15
		15.60	EB sampling, $\gamma = 1.0$	—	81	16	117.21	91.31
	BLT-DV (diffusion+verification)	19.00	Confidence-based, $\alpha = 0.3$	74.77	56	41	251.34	81.37
			EB sampling, $\gamma = 1.5$	81.05	107	37	250.43	81.44
			EB sampling, $\gamma = 2.0$	80.38	97	38	249.14	81.54
			one step	71.79	42	42	255.40	81.07